EVALUATION OF THE ACCURACY OF EQUIVALENT LINEAR ANALYSIS METHOD FOR SEISMIC ISOLATED BUILDINGS

A THESIS SUBMITTED TO
THE GRADUATE SCHOOL OF NATURAL AND APPLIED SCIENCES
OF
MIDDLE EAST TECHNICAL UNIVERSITY

BY

SEZER MUTLU

IN PARTIAL FULFILLMENT OF THE REQUIREMENTS
FOR
THE DEGREE OF MASTER OF SCIENCE
IN
ENGINEERING SCIENCES

DECEMBER 2021

Approval of the thesis:

EVALUATION OF THE ACCURACY OF EQUIVALENT LINEAR ANALYSIS METHOD FOR SEISMIC ISOLATED BUILDINGS

submitted by **SEZER MUTLU** in partial fulfillment of the requirements for the degree of **Master of Science** i**n Engineering Sciences, Middle East Technical University** by,

Prof. Dr. Halil Kalıpçılar
Dean, Graduate School of **Natural and Applied Sciences** _____

Prof. Dr. Murat Dicleli
Head of the Department, **Engineering Sciences** _____

Prof. Dr. Murat Dicleli
Supervisor, **Engineering Sciences, METU** _____

Examining Committee Members:

Assoc. Prof. Dr. Ferhat Akgül
Engineering Sciences, METU _____

Prof. Dr. Murat Dicleli
Engineering Sciences, METU _____

Prof. Dr. Tolga Akış
Civil Engineering, Atılım University _____

Date: 01.12.2021

I hereby declare that all information in this document has been obtained and presented in accordance with academic rules and ethical conduct. I also declare that, as required by these rules and conduct, I have fully cited and referenced all material and results that are not original to this work.

Name Last name : Sezer Mutlu

Signature :

ABSTRACT

EVALUATION OF THE ACCURACY OF EQUIVALENT LINEAR ANALYSIS METHOD FOR SEISMIC ISOLATED BUILDINGS

Mutlu, Sezer
Master of Science, Engineering Sciences
Supervisor : Prof. Dr. Murat Dicleli

December 2021, 75 pages

Earthquakes have been the leading cause of loss of lives and properties since the beginning of human history. After major earthquakes, we see that even the buildings constructed using modern engineering solutions suffer severe damage or even collapse. Seismic base isolation systems are used to minimize earthquake-induced damage. This thesis focuses on evaluating the accuracy of the equivalent linear analysis method in the analysis of seismic base-isolated buildings. In order to do that, certain buildings with different story numbers, widths, and isolator parameters were analyzed by using a set of ground motions selected for different soil properties, and results were compared with the results obtained from the equivalent linear analysis method.

Keywords: Equivalent Linear Analysis, Time History Analysis, Seismic Base Isolation, Earthquake, Friction Pendulum Bearing

ÖZ

DEPREM YALITIMLI BİNALAR İÇİN EŞDEĞER DOĞRUSAL ANALİZ YÖNTEMİNİN DOĞRULUĞUNUN DEĞERLENDİRİLMESİ

Mutlu, Sezer
Yüksek Lisans, Mühendislik Bilimleri
Tez Yöneticisi: Prof. Dr. Murat Dicleli

Aralık 2021, 75 sayfa

Depremler, insanlık tarihinin başından beri en fazla can ve mal kaybına yol açan olayların başında gelmektedir. Büyük depremler sonrasında, günümüzün gelişmiş mühendislik çözümleri kullanılarak inşa edilen binalarının bile ciddi hasarlar aldığını, kimi zaman ise yıkıldığını görülmektedir. Sismik taban izolasyon sistemleri ise deprem kaynaklı hasarları en aza indirmek için kullanılmaktadır. Bu tez çalışması, deprem izolasyonlu binaların analizinde, eşdeğer doğrusal analiz yönteminin doğruluğunu değerlendirmeye odaklanmaktadır. Bunu yapabilmek için farklı izolatörler üzerindeki, belirli kat ve genişliklerde seçilen binalar, farklı zemin tiplerine göre seçilen ve farklı şiddetlerdeki zaman tanım aralığı depremleri altında analiz edilmiş ve bulunan sonuçlar eşdeğer doğrusal analiz yönteminden elde edilen sonuçlarla karşılaştırılmıştır.

Anahtar Kelimeler: Eşdeğer Doğrusal Analiz, Zaman Tanım Alanında Analiz, Sismik Taban İzolasyonu, Deprem, Sürtünmeli Sarkaç İzolatör

Dedicated to my Family

ACKNOWLEDGMENTS

First of all, I would like to express my deepest gratitude to my supervisor Prof. Dr. Murat Dicleli, for the help he provided with his endless experience and great engineering knowledge. His advice, criticism, and opinions added significant value to the research.

Secondly, I would like to thank Assoc. Prof. Dr. Mustafa Tolga Yılmaz for his unconditional support and valuable ideas.

I would also like to thank my friends Oğuz Zerman, Çağrı İmamoğlu, Tareq Rabaia, Burhan Buğrahan Puhurcuoğlu and Pourya Tabiehzad for their suggestions, comments and also for their friendship.

Last but not least, I would like to thank my parents and brothers for their support and love.

Finally, I would like to thank my wife Bengü Macit Mutlu for her endless patience, care, and love.

TABLE OF CONTENTS

LIST OF TABLES

TABLES

LIST OF FIGURES

FIGURES

CHAPTER 1

INTRODUCTION

1.1 Introduction

Earthquakes are one of the biggest challenges facing civil engineers. Design codes that have been proposed by various organizations in different countries aim to help engineers to design earthquake-resistant structures. Engineers' duty is to design cost-effective structures while following these design codes. The main objective is to avoid collapse to prevent loss of life for residential buildings. On the other hand, essential facilities such as hospitals, administrative buildings, fire stations, and communication centers are required to remain fully functional after an earthquake. In order to achieve this, the building should remain undamaged and floor accelerations should be limited. In this sense, earthquake isolation systems are vital tools to reduce earthquake induced damages and keep the building fully functional.

During an earthquake, if the period of the earthquake matches the period of the building, the possibility of having severe damage increases resulting in partial or total collapse. This phenomenon is called resonance. Seismic isolation systems decrease the resonance possibility by increasing the building period. In addition, spectral acceleration generally reduces as the period of structure increases. In a conventional structure, earthquake loads are directly transferred from the foundation to columns and beams. Seismic base isolation devices aim to separate the foundation from the superstructure and allow them to move separately. Base-isolated structures can be analyzed with Time History Anaylsis (THA). However, this method takes much longer time due to the nonlinear behavior. On the other hand, Equivalent Linear Analysis (ELA) can also be used to analyze base-isolated structures. This

method offers a much faster solution compared to THA. ASCE 7-16 and Turkish Earthquake Code require both ELA and THA to compare the base shear and displacement results at specified rates.

As mentioned in the literature review section, several research studies have been done to provide reliable comparisons between the two methods. However, most of these studies are conducted using single-degree of freedom (S-DOF) systems.

In this study, both single-degree of freedom (S-DOF) and multi-degree of freedom (M-DOF) systems are used to model structures isolated at their base using the Friction Pendulum System (FPS). These models are analyzed by performing THA and ELA. The results of the two methods are compared, and the accuracy of ELA is evaluated. Furthermore, Friction Pendulum Bearings are modeled using "Friction Isolator" model and "Plastic-Wen" model, and the results of the two models obtained from THA are also compared.

1.2 Objective and Scope

The main objective of this study is evaluating the accuracy of the equivalent linear analysis method for the base-isolated structures by comparing the results of the equivalent linear analysis method with time history analysis method. This study focuses on reinforced concrete structures isolated with friction pendulum bearings. Moreover, the effects of various parameters such as the number of stories, number of bays, soil type, isolator friction, and radius of curvature on the results are also be examined within the scope of the study.

1.3 Literature Review

Several studies have been conducted to evaluate the accuracy of equivalent linear analysis for SDOF structures or simplified MDOF structures on different types of isolators.

Dicleli & Buddaram (2007) investigated the effect of parameters such as the intensity and frequency characteristics of the ground motion, isolator properties, and the structure mass for SDOF systems. Analyses were performed for seismic-isolated structures represented by isolators placed on rigid supports which supporting a rigid mass. Hence, the variables were isolator properties, ground motion properties, and the mass of the structure. It was found that the ratio of the peak ground acceleration to peak ground velocity of the ground motion affects the accuracy of the equivalent linear analysis results as well as the intensity of the ground motion relative to the characteristic strength of the isolator. Several improvements were proposed for effective damping equation used in the design of seismic isolated structures and analysis procedure for more accurate predictions.

Ozdemir & Constantinou (2010) evaluated the accuracy of the displacements and shear forces estimated by the equivalent linear method. A 3-story reinforced concrete structure supported by 20 isolators was analyzed. The study concluded that the equivalent linear method may underestimate or overestimate the displacements and base shear forces up to 12% and 15%, respectively. Since these differences were considered to be within acceptable limits, it was interpreted that the equivalent linear method predicted conservative results.

Liu et al. (2014a) performed equivalent linear and time history analysis using seven ground motion records which scaled to the target spectrum. A 5-story reinforced concrete structure isolated by the friction pendulum system was used to evaluate the accuracy of the equivalent linear method. The study concluded that displacements were overestimated by the equivalent linear method by 10% compared with the average results of the nonlinear analysis method, which was considered as a

conservative estimate. However, the equivalent linear method estimated unconservative results for story shear force. Base shear force was slightly overestimated by the equivalent linear method. On the other hand, shear forces in the upper floors were significantly underestimated, which was caused by the uniform acceleration profile over the height of the building.

Liu et al. (2014b) also studied on the improvement of the equivalent linear method. A factor "F" was introduced to modify the equivalent viscous damping ratio. The proposed ELA model has improved the estimation accuracy of ELA method.

Alhan & Özgür (2015) investigated the accuracy of equivalent linear analysis via numerical experiments conducted on 3D, five-story, seismically isolated buildings. In this study, elastomeric isolators were used as isolation system. In addition, near-fault earthquake records were used. Isolation system displacements, roof accelerations, story drifts, base shears, and torsional base moments from equivalent linear analysis and time history analysis were compared. It was found that the equivalent linear approach produces better estimates of peak base displacements and peak torsional base moments as the effective periods of seismic-isolation systems and rigid-body mode periods gets smaller. In addition, it was also found that the equivalent linear approach results in better estimates of all structural response parameters when the effective viscous damping ratio of the seismic-isolation system is smaller, and the post-yield to pre-yield stiffness ratio is higher. The study was concluded that the equivalent linear method results in conservative estimates of peak top floor acceleration, peak first story drift ratios, and peak base shears. However, it results in unconservative estimates of peak base displacements and peak torsional base moments.

Simon et al. (2015) evaluated the equivalent linear method for the seismic retrofit design of Haros M0 Highway Bridge. The results showed that the force in the isolation system could be approximated with negligible error. However, the accuracy of the equivalent linear method is not sufficient for pier moment, deformation, displacement, and element force results.

Kim (2017) evaluated the equivalent linear method for seismic response analysis of base-isolated structures. In this study, forty ground motions were selected and scaled to the target response spectra for NEHRP site category S_d. Time history analyses and equivalent linear analyses were conducted for 5-story structure with 3 m story height, which idealized as a 6-DOF system. Relative displacement and absolute acceleration were taken as main indicators to investigate the damage of structural and non-structural members, respectively. Displacement and acceleration values for each story were obtained, and the error percentage was calculated for every story. It was concluded that the ELA method can be considered as a reliable analysis method for relative displacement. On the other hand, ELA method was found as an insufficient method for estimation of absolute acceleration response. The reason for the underestimation of absolute acceleration response was attributed to the inability of ELA method to reflect the structural mode as the nonlinear method.

Nguyen & Dao (2021) evaluated the accuracy of the peak displacement predicted by an equivalent linear model isolated by friction pendulum bearings. The system was modeled as a single mass with bidirectional movement in-plan. The nonlinear isolation system was modeled with a friction pendulum element with a velocity-dependent friction coefficient ranging from 0.02 to 0.16. The secant stiffness at peak displacement was used as the stiffness of the corresponding equivalent linear model. The study concluded that the equivalent linear method underestimates the displacements at small displacements and overestimates the displacements at large displacements. It is also stated that ground motions with pulse produce larger peak displacements. It is observed that the equivalent linear method can underestimate displacements by half or overestimate it up to 100%. However, when a graph is prepared with a large number of data, it was seen that the data points generally gather along a line, which implies that the equivalent linear method can partially predict the peak displacement.

1.3.1 Isolator Parameters

Lousidis (2015) investigated the effectiveness of seismic isolation systems by comparing the time history analysis results with the fixed-based case. Friction pendulum bearings were used with an initial stiffness equal to 100 times of post stiffness.

Siciliano (2016) studied elastomeric rubber bearings and friction pendulum systems. Initial stiffness to post stiffness ratio for FPS was taken between 50 and 100. Gino et al. (2020) studied retrofitting of existing reinforced concrete structure using friction pendulum devices, using initial stiffness equal to $51k_p$.

1.3.2 Structural Damping of Base-Isolated Structures

Since the energy dissipation in the structural members of a base-isolated structure is less than a conventional structure, it would be a reasonable approach to take the damping coefficient lower than the frequently used value of 5%. Nagarajaiah et al. (1991) studied the nonlinear dynamic analysis of 3D base-isolated structures and compared the results with experimental results. In this study, a damping ratio of 2% of critical was used for the superstructure, and consistent results were obtained.

Ryan & Polanco (2008) studied Rayleigh damping in base-isolated buildings. It is stated that the first mode and some higher mode of the structure, which will include the majority of the modal participation, is selected for the mass and stiffness proportional damping calculation. In addition, a damping ratio of 5% or less of the critical would be a reasonable value for the corresponding damping ratio.

Pant et al. (2013) studied viscous damping appropriate for the nonlinear time-history analysis of base-isolated reinforced concrete buildings, and a smaller damping ratio of 1% was found to be more appropriate instead of the commonly used value of 5%.

Based on the literature review, a damping ratio of 2% is used in this study.

CHAPTER 2

STUDY PARAMETERS AND ANALYSIS MODEL

The analysis model and analysis parameters are presented in this chapter. 2D portal frames with different bay and story numbers are used in this study. Since hospitals are one of the buildings where seismic base isolation is most commonly used, in this study, the buildings are considered as hospitals and the loads are calculated accordingly. In addition, several parameters are selected to evaluate the accuracy of equivalent linear analysis. These parameters can be grouped as isolator parameters, parameters selected for the structure, and soil parameters.

2.1 Isolator Parameters

Friction pendulum (FPS) bearing is used in this study. A typical friction pendulum bearing and its properties affecting isolator stiffness are presented in Figure 2.1.

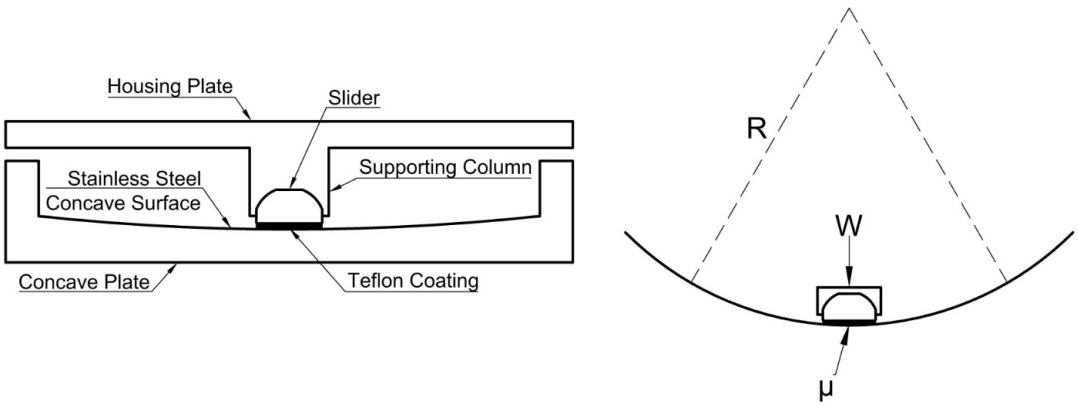

Figure 2.1. Friction Pendulum Bearing

In order to evaluate the accuracy of equivalent linear analysis for different FPS isolators, radius of curvature (R=3m, 5m, 7m) and friction coefficient values (μ = 0.03, 0.05, 0.07) are selected. In addition, 5m curvature radius and 5% friction coefficient are selected as benchmark values. Selected isolator parameters are shown in Table 2.1.

Table 2.1 Selected Isolators

Isolators	*R (m)*	*μ (%)*
1	3	5
2	5	3
3 (Benchmark)	5	5
4	5	7
5	7	5

2.2 Parameters Selected for the Structure

2D portal frames with different story numbers and bays are used in this study. Materials are selected as C40/45 for reinforced concrete and S420 for rebars. In order to evaluate the accuracy of equivalent linear analysis method for structures with different degree of freedom numbers, buildings with 2, 4, 8, 12-story, and 3, 5, 7-bay are selected. 8-story and 5-bay selected as benchmark values. Properties of buildings are presented in Table 2.2.

Table 2.2 Selected Buildings

Buildings	*Number of Bays*	*Number of Stories*
1	3	8
2	5	2
3	5	4
4 (Benchmark)	5	8
5	5	12
6	7	8

Story height and width of the bays are selected as 3m and 6m, respectively. The benchmark building and the typical building used in this study is presented in Figure 2.2 and Figure 2.3, respectively.

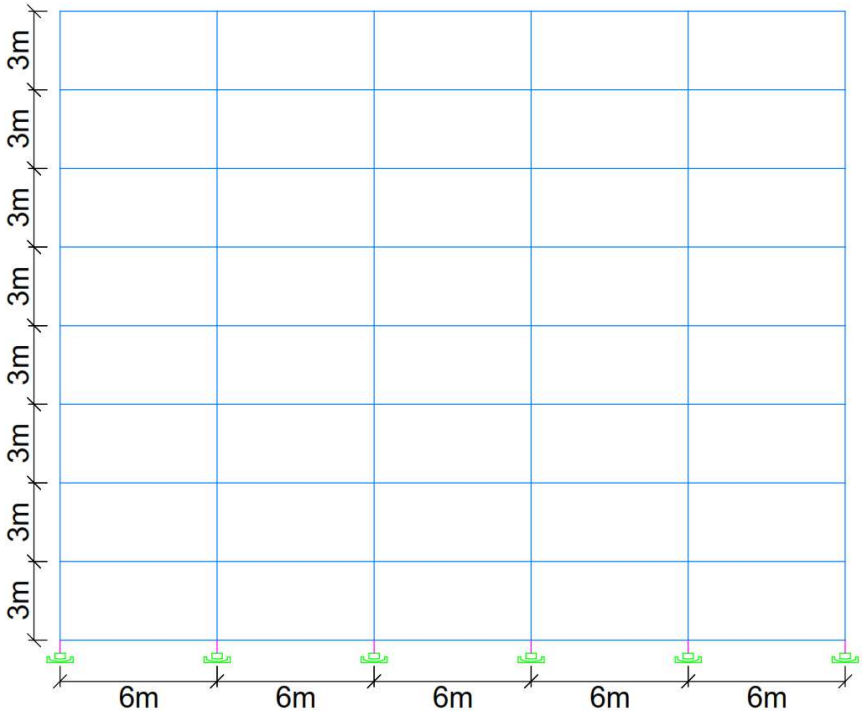

Figure 2.2. Benchmark Building

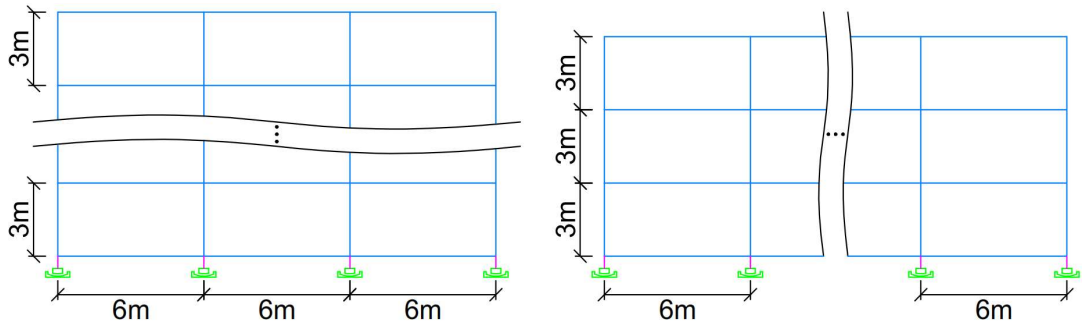

Figure 2.3. The Typical Building

2.3 Soil Parameters and Peak Ground Accelerations

In order to evaluate the accuracy of equivalent linear analysis on different soil sites, three different soil sites (Site Class B - Site Class C - Site Class D) are selected for the analysis. For each soil site, a set of seven ground motions are selected, and 2% damped response spectra of each ground motion are calculated and scaled to selected PGA values, which are determined as 0.25 (g), 0.50 (g), and 0.75 (g). Therefore, nine ground motion sets are obtained.

2.4 Loads

Dead and live loads are calculated according to ASCE/SEI 7-16 (2017), considering that the building is a hospital. The density of reinforced concrete is selected as 23.6 kN/m³ from ASCE/SEI 7-16 (2017), Table C3.1-2. The thickness of the slab is taken 30cm for isolation level and 15cm for other stories. Calculation of dead load for isolation level, regular stories, and roof level is presented in Table 2.3.

Table 2.3 Dead Load

Load Source	Isolation Level	Regular Story	Roof
	Load (kN/m²)	Load (kN/m²)	Load (kN/m²)
Cement Finish (25mm)	1.53	1.53	1.53
Ceramic on 25mm mortar bed	1.1	1.1	1.1
Suspended Metal Lath and Cement Plaster	0.72	0.72	0.72
Partition Wall	0.77	0.77	0
Slab (15cm)	-	3.54	3.54
Slab (30cm)	7.08	-	-
Total	11.2	7.66	6.89

In order to determine live loads, firstly, the floor plans of the existing hospitals were examined, and the ratio of the corridors to the total plan area was calculated, and 25 percent was accepted. According to ASCE/SEI 7-16 (2017), Table 4.3-1, uniformly distributed loads are taken as 2.87 kN/m² for operating rooms or laboratories, 1.92 kN/m² for patient rooms, and 3.83 kN/m² for corridors. The first story of the 2-story hospital and the first two story of 4-8-12-story hospitals are considered as laboratories and operating rooms. The rest of the stories are considered as patient rooms. The calculation of the distributed live loads for 25% corridor ratio is presented in Table 2.4.

Table 2.4 Live Load

Load Location	Load (75%) (kN/m³)	Corridor Load (25%) (kN/m³)	Final Load (kN/m³)
Operating Rooms, Laboratories	2.87	3.83	3.11
Patient Rooms	1.92	3.83	2.3975

Slabs are assumed as two-way, and load distributions are calculated accordingly. Since the analysis models are prepared in 2D, the loads transferred from out-of-plane

slabs and beams are calculated for half of the span length on both sides and applied as a point or distributed load to the beams and columns, as shown in Figure 2.4.

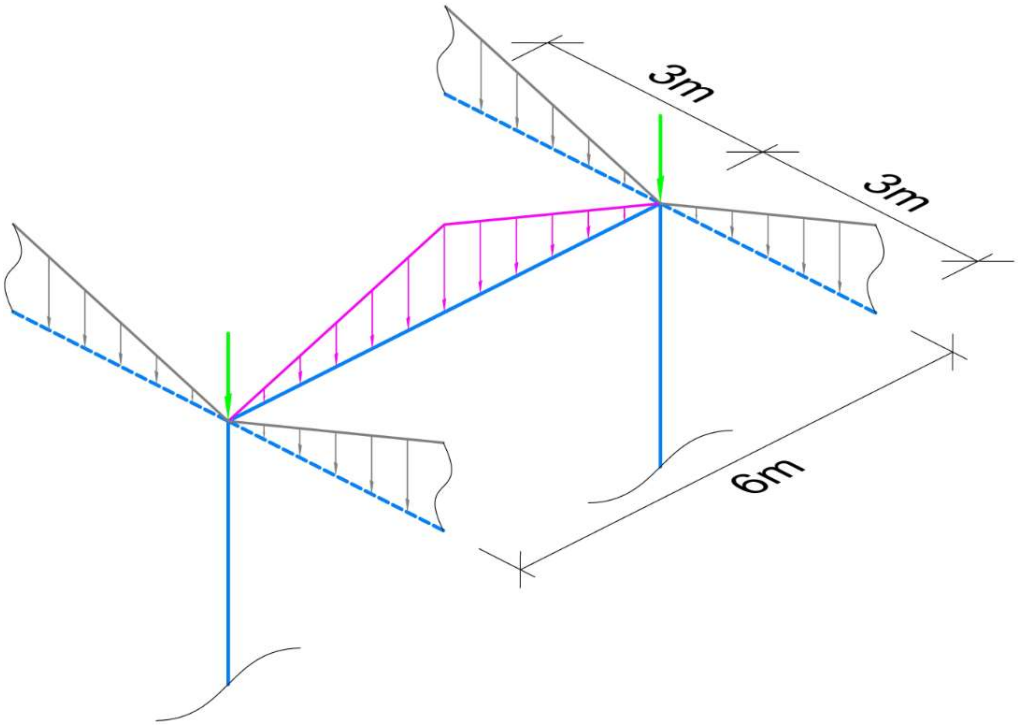

Figure 2.4. Distributed and point loads (Gray: Distributed loads on the out-of-plane beams, Green: Sum of gray load and dead load of out-of-plane beams, Magenta: Distributed load from slabs)

2.5 Modeling

Base models are constructed using CSI SAP2000 v22 (2020) for the selected buildings. Square sections with different dimensions are used for columns, and beams with T shape are used to be able to get more realistic behavior. Column and beam dimensions are shown in Table 2.5.

Table 2.5 Column and Beam Dimensions

Story Number	Column Dimensitons (cm)				Beam Dimensitons (cm)			
	2 story	4 story	8 story	12 story	2 story	4 story	8 story	12 story
1	45x45	60x60	75x75	90x90	40x60	40x60	40x70	40x70
2	45x45	60x60	75x75	90x90	40x60	40x60	40x70	40x70
3	-	60x60	75x75	90x90	-	40x60	40x70	40x70
4	-	60x60	75x75	90x90	-	40x60	40x70	40x70
5	-	-	60x60	75x75	-	-	40x60	40x70
6	-	-	60x60	75x75	-	-	40x60	40x70
7	-	-	60x60	75x75	-	-	40x60	40x70
8	-	-	60x60	75x75	-	-	40x60	40x70
9	-	-	-	60x60	-	-	-	40x60
10	-	-	-	60x60	-	-	-	40x60
11	-	-	-	60x60	-	-	-	40x60
12	-	-	-	60x60	-	-	-	40x60

Bearings are placed under 0.5 m of isolation level beam to consider the thickness of the isolation level beam to make the analysis model more realistic. In order to model the friction pendulum bearings for equivalent linear analysis, linear springs with equivalent stiffness (k_e) are used, as shown in Figure 2.5. Equivalent stiffness (k_e) is calculated using maximum displacement (D_d) as follows:

$$F_{yi} = \mu W \tag{2.1}$$

$$k_p = \frac{W}{R} \tag{2.2}$$

$$k_e = \frac{F_d}{D_d} = \frac{F_{yi}}{D_d} + k_p \tag{2.3}$$

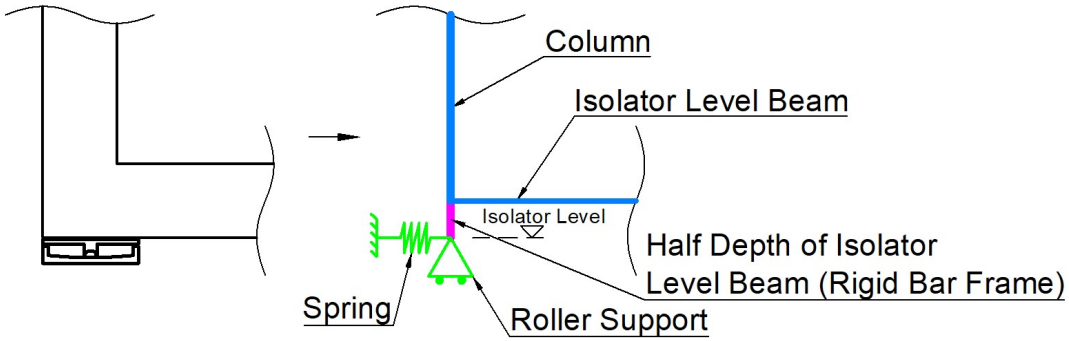

Figure 2.5. Modeling of FPS for Equivalent Linear Analysis

Two types of link properties are used to model the hysteresis loop for time history analysis in order to examine possible differences. The first link type is "Friction Isolator" and the second link type is "Plastic-Wen". These two link properties require similar isolator properties such as yielding force (F_y), initial stiffness (k_i), post stiffness (k_p), or their ratio (k_i/k_p). Modeling of friction pendulum system as friction isolator for time history analysis is presented in Figure 2.6.

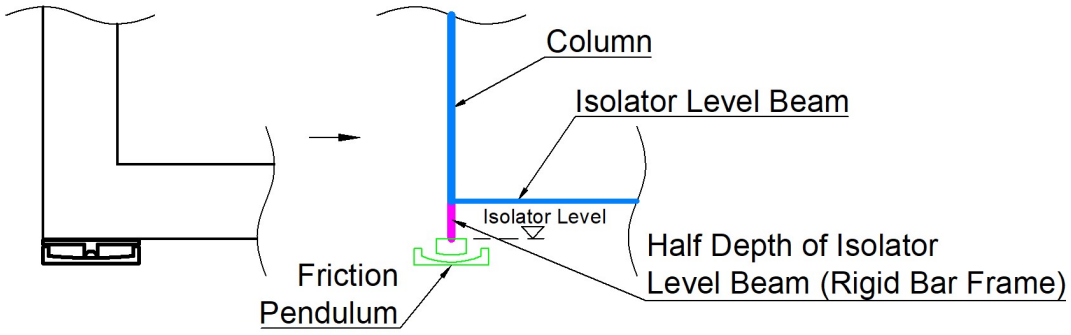

Figure 2.6. Modeling of FPS for Time History Analysis

Initial stiffness (k_i) is expressed as a ratio to post stiffness (k_i/k_p). In order to get a closer approach to the real behavior, previous studies with friction pendulum bearing have been examined, and it has been found that this ratio is generally taken between 50 and 100. In addition, experiment logs of several manufacturers are examined, and this ratio is taken as 50 for this study.

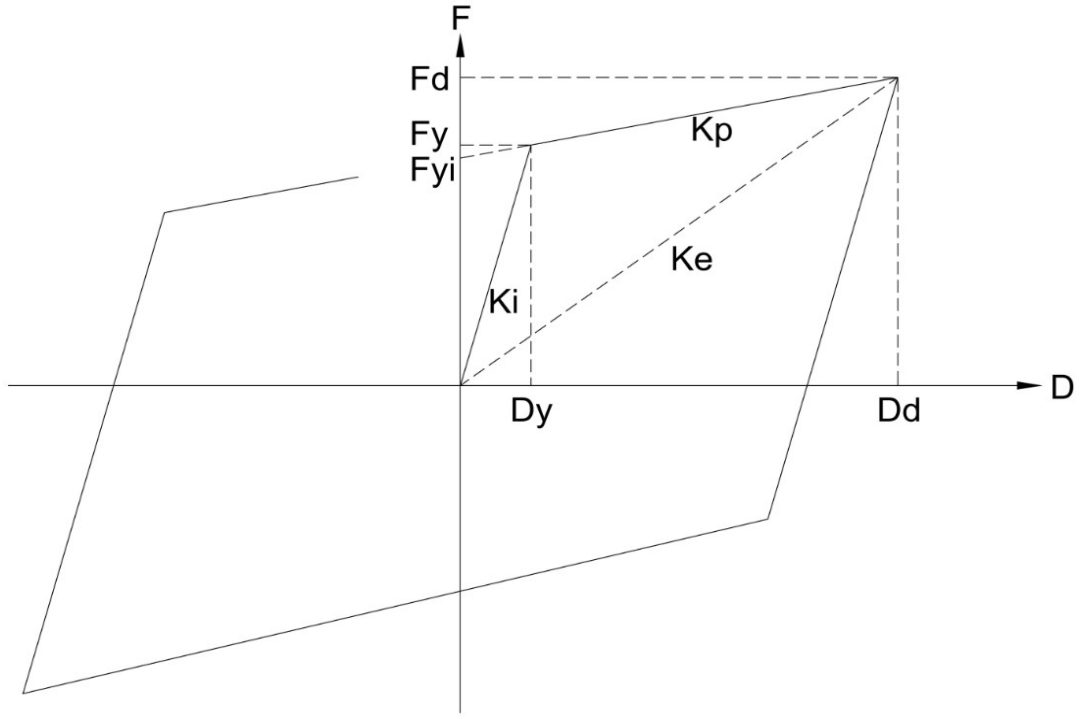

Figure 2.7. Hysteresis Loop

CHAPTER 3

SELECTION AND SCALING OF TIME HISTORY RECORDS AND CONSTRUCTION OF RESPONSE SPECTRUM

3.1 Selection of Ground Motions

Three different sets of ground motion records are selected for each soil site class, and each set consists of seven ground motion records. These records are selected from Peer Ground Motion database by limiting the distance to the rapture between 20 and 75 kilometers. Records are selected for soil types B, C, and D using average shear wave velocity for the top 30m (Vs^{30}). Boundaries for B, C, and D soil types are selected as 720-1500 m/s, 360-720 m/s, and 180-360 m/s, respectively.

Selected ground motion sets for soil site classes B, C, and D are presented in Table 3.1, Table 3.2 and

Table 3.3, respectively.

Table 3.1 Ground Motion Set Selected for Soil Site Class B

GM ID	Rec. Seq. Number	Earthquake	Station Name	Magnitude	Rrup (km)
1	788	Loma Prieta	Piedmont Jr High School Grounds	6.93	73
2	797	Loma Prieta	SF - Rincon Hill	6.93	74.14
3	989	Northridge-01	LA - Chalon Rd	6.69	20.45
4	1011	Northridge-01	LA-Wonderland Ave	6.69	20.29
5	1347	Chi-Chi Taiwan	ILA063	7.62	61.06
6	2753	Chi-Chi Taiwan-04	CHY102	6.2	39.32
7	5487	Iwate Japan	MYGH12	6.9	57.19

Table 3.2 Ground Motion Set Selected for Soil Site Class C

GM ID	Rec. Seq. Number	Earthquake	Station Name	Magnitude	Rrup (km)
1	787	Loma Prieta	Palo Alto - SLAC Lab	6.93	30.9
2	963	Northridge-01	Castaic-Old Ridge Route	6.69	20.7
3	1476	Chi-Chi Taiwan	TCU029	7.62	28
4	1762	Hector Mine	Amboy	7.13	43.1
5	4874	Chuetsu-oki Japan	Oguni Nagaoka	6.8	20
6	5663	Iwate Japan	MYG004	6.9	20.2
7	6915	Darfield New Zealand	Heathcote Valley Primary School	7	24.5

Table 3.3 Ground Motion Set Selected for Soil Site Class D

GM ID	Rec. Seq. Number	Earthquake	Station Name	Magnitude	Rrup (km)
1	169	Imperial Valley-06	Delta	6.53	22.03
2	776	Loma Prieta	Hollister-South&Pine	6.93	27.93
3	900	Landers	Yermo Fire Station	7.28	23.62
4	1183	Chi-Chi Taiwan	CHY008	7.62	40.43
5	3749	Cape Mendocino	Fortuna Fire Station	7.01	20.41
6	5991	El Mayor-Cucapah Mexico	El Centro Array #10	7.2	20.05
7	6966	Darfield New Zealand	Shirley Library	7	22.33

3.1.1 Scaling

Firstly selected ground motion records are converted to 2% damped spectra. Since PEER Ground Motion Database only calculates 5% damped spectra, a program is developed using Newmark's Step by Step Integration algorithm in order to calculate 2% damped spectra. After 2% damped spectra are calculated, the peak ground acceleration (PGA) of each spectra is scaled to 0.25g, 0.50g, and 0.75g. Finally, 3 sets are obtained from different soil classes, and 3 sets are obtained from different PGA values for each soil class. Therefore, nine ground motion sets are obtained.

3.2 Construction of Smoothed Response Spectrum

The average spectrum of 7 scaled ground motion spectra is calculated for each ground motion set for different soil types and PGA values. Then a smoothed spectrum is fitted to the average spectrum of the each ground motion set. Each smoothed response spectrum function is composed of three regions; (i) ascending region (acceleration sensitive region), flat region (displacement sensitive region), descending (displacement sensitive region). The ascending region of the smoothed response spectrum is obtained by fitting a minimum least square linear function to the average spectrum within that region. Then, the spectral amplitude of the flat region is defined as the weighted average of the related region. Finally, a minimum least square power function is fitted to the descending part of the average response spectrum. Smoothed response spectrum functions constructed for soil type B, C, and D are shown in Figure 3.1, Figure 3.2, Figure 3.3, respectively. These functions are obtained for a PGA value of 0.25g. For other PGA values used, response spectrum functions are simply multiplied by 2 and 3 for 0.50g and 0.75g, respectively. Therefore, 9 constructed response spectrum functions are obtained for each site class B, C, and D and each PGA value. Equivalent linear analyses are conducted with these constructed response spectrum functions.

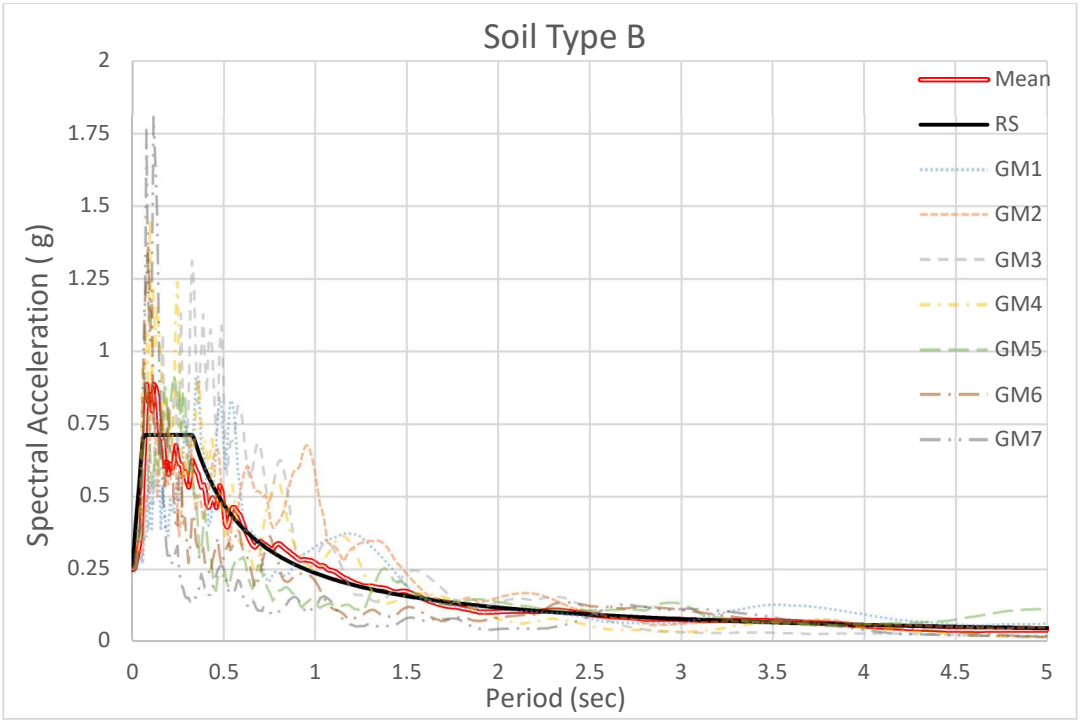

Figure 3.1. Response Spectrum Constructed for Soil Type B

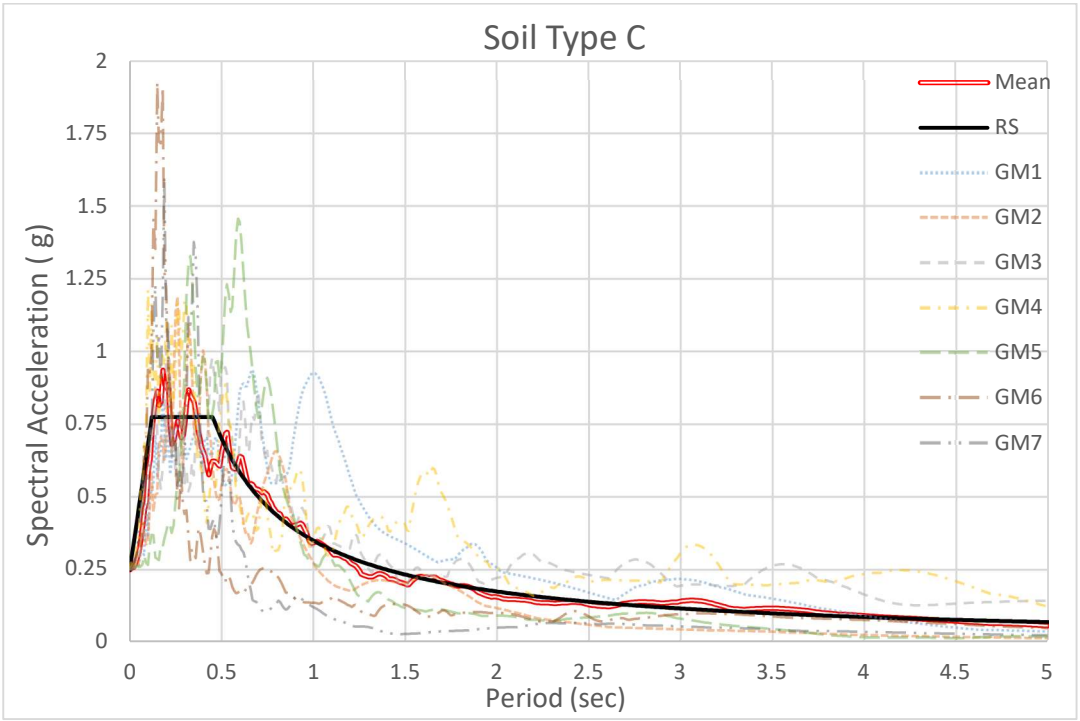

Figure 3.2. Response Spectrum Constructed for Soil Type C

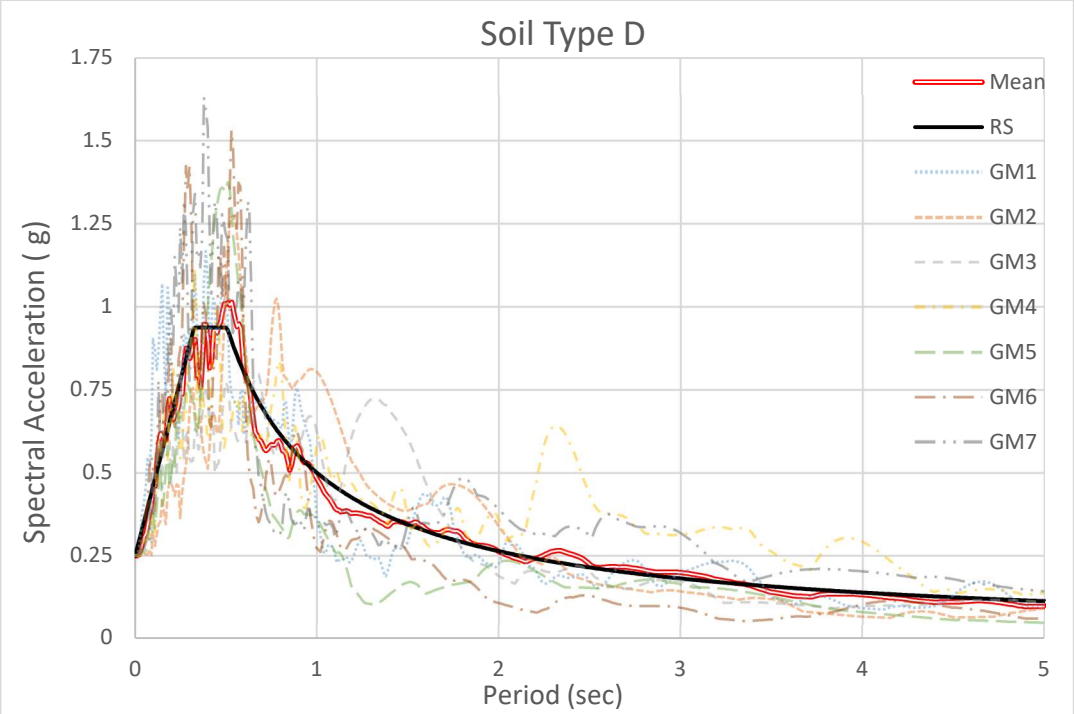

Figure 3.3. Response Spectrum Constructed for Soil Type D

CHAPTER 4

ANALYSIS METHODS

4.1 Equivalent Linear Analysis Method

An iterative procedure was followed in the analyses performed with the equivalent linear analysis method. Dicleli & Buddaram (2007) indicated the steps of the iterative procedure commonly followed for the design of seismic isolated structures as follows;

Step 1: Assume a design displacement (U_d) for the isolator.

Step 2: Calculate the effective stiffness (k_e) of the isolator from Eq. (4.1). The variables in Eq. (4.1) are shown in Figure 2.7.

Step 3: Calculate the equivalent viscous damping ratio (ζ_e) from Eq. (4.2) and limit the effective viscous damping ratio (ζ_e) between 5% and 30%.

Step 4: Calculate the effective period (T_e) of the seismic-isolated structure from Eq. (4.3).

Step 5: Calculate the damping reduction factor, B, from Eq. (4.4), which is used in AASHTO (2014), and construct the response spectrum.

Step 6: Obtain a new design displacement (U_d) and compare it with the previous one. If the difference is smaller than a predetermined tolerance level, terminate the iteration. Otherwise, go to step 2 to continue with the next round of iterations using the new design displacement.

Dicleli & Mansour (2003) derived Eq. (4.2) to calculate the equivalent viscous damping ratio (ζ_e) for the friction pendulum bearings. The effect of limiting the equivalent viscous damping coefficient specified in step 3 will also be examined in Chapter 6.

$$k_e = \frac{F_d}{D_d} = \frac{F_{yi}}{D_d} + k_p \tag{4.1}$$

$$\zeta_e = \frac{2}{\pi}\left(\frac{\mu}{\mu + (D_d/R)}\right) \tag{4.2}$$

$$T_e = 2\pi\sqrt{\frac{m}{k_e}} \tag{4.3}$$

$$B = \left(\frac{\zeta_e}{0.05}\right)^3 \tag{4.4}$$

The calculation of the 2% damped response spectrum was explained in Chapter 2. The spectral accelerations of the 2% damped response spectrum are used for periods smaller than 80% of the effective period (0.8 T_e). Since Eq. (4.4) is constructed for 5% damping ratio, the 5% damped response spectrum is also constructed, and this spectrum is reduced by dividing the damping reduction factor (B), and is used for periods greater than 80% of the effective period (0.8 T_e).

80% of the effective period (0.8 T_e) is used to separate the isolation modes from the other modes. The periods of the isolation modes are greater than the specified limit, while the periods of the other modes are smaller. In other words, the damping reduction factor (B) is only used for the isolation modes.

Within the scope of the study, a total of 270 analyses were conducted with the equivalent linear method.

4.2 Time History Analysis Method

4.2.1 Modeling The Hysteresis Loop of The Bearing

As mentioned in Chapter 2, two types of link properties are used to model the hysteresis loop. The first link type is “Friction Isolator” and the second link type is “Plastic-Wen”. Since the initial stiffness (k_i), yield force (F_y) and the post stiffness (k_p) are defined as constant values for “Plastic-Wen” link type, a bilinear hysteresis loop will be formed. However, in real case, because the axial load will change during an earthquake, the isolator stiffness will also change and a fluctuated hysteresis loop will be formed. This behavior is modeled with “Friction Isolator” link type. In total, 270 analyses are conducted with each isolator type.

4.2.2 Time History Records

The selection and scaling of ground motion records were explained in Chapter 3. In order to obtain compatible results with the equivalent linear method, mass and stiffness proportional damping coefficients are calculated from the period values and the corresponding damping ratios, as shown in Figure 4.1. The first two periods with the highest modal mass participation ratio are used as the first and second periods with a corresponding damping ratio of 2%.

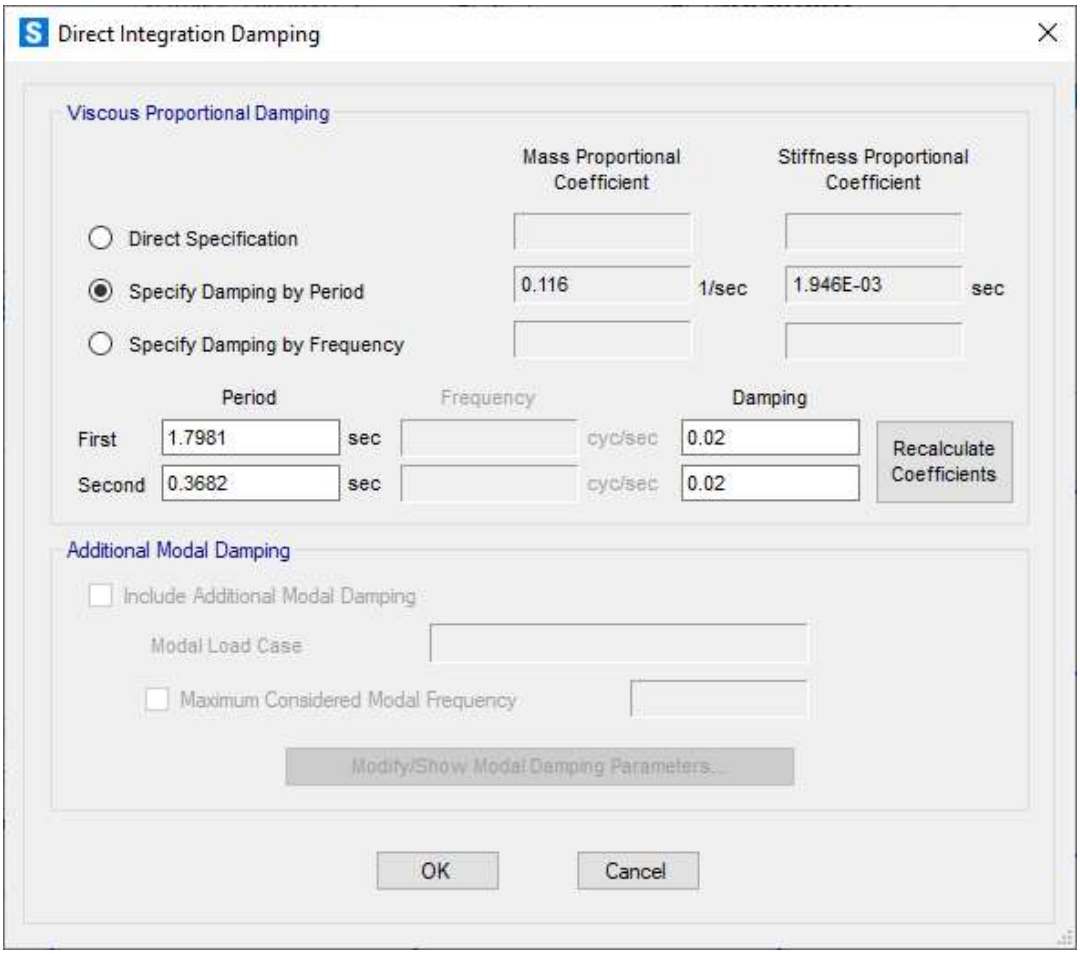

Figure 4.1. Calculation of Mass and Stiffness Proportional Damping

CHAPTER 5

SENSITIVITY ANALYSES

5.1 Effect of Hysteresis Loop Type on Results

5.1.1 Introduction

In this section, the effects of different types of link properties on the nonlinear analysis results are investigated. The hysteresis loop of the isolation system is modeled with both Friction Isolator link and Plastic-Wen link. The isolator parameters such as friction coefficient (μ), and pendulum radius (R) are specified for Friction Isolator link type. On the other hand, the yielding force (F_y) and the post stiffness (k_p) are defined as constant values for Plastic-Wen link type. In addition, the yield exponent is taken as 22 for Plastic-Wen.

5.1.2 Evaluation of the Results

5.1.2.1 Base Reactions

In total, 270 models for both Friction Isolator and Plastic-Wen link types are analyzed. Then the percentage difference between the two results is calculated. The results are presented as the number of models within specific percentage variation ranges. The total area represents 270 analysis models for all charts. The results of base shear, base moment, isolator level acceleration, and isolator level displacement are presented in Figure 5.1.

As seen in the graphs, the highest variation is observed in the base shear results. Out of 270 analysis models, the difference is less than 2% for 105 models, between 2%-5% for 135 models, and between 5%-10% for 27 models. However, the percentage

difference is smaller than 2% for 262 and 251 analysis models according to the base moment and the isolator level acceleration results, respectively. Much more consistent results are obtained for the isolator level displacements, since the percentage difference is less than 1% for all models.

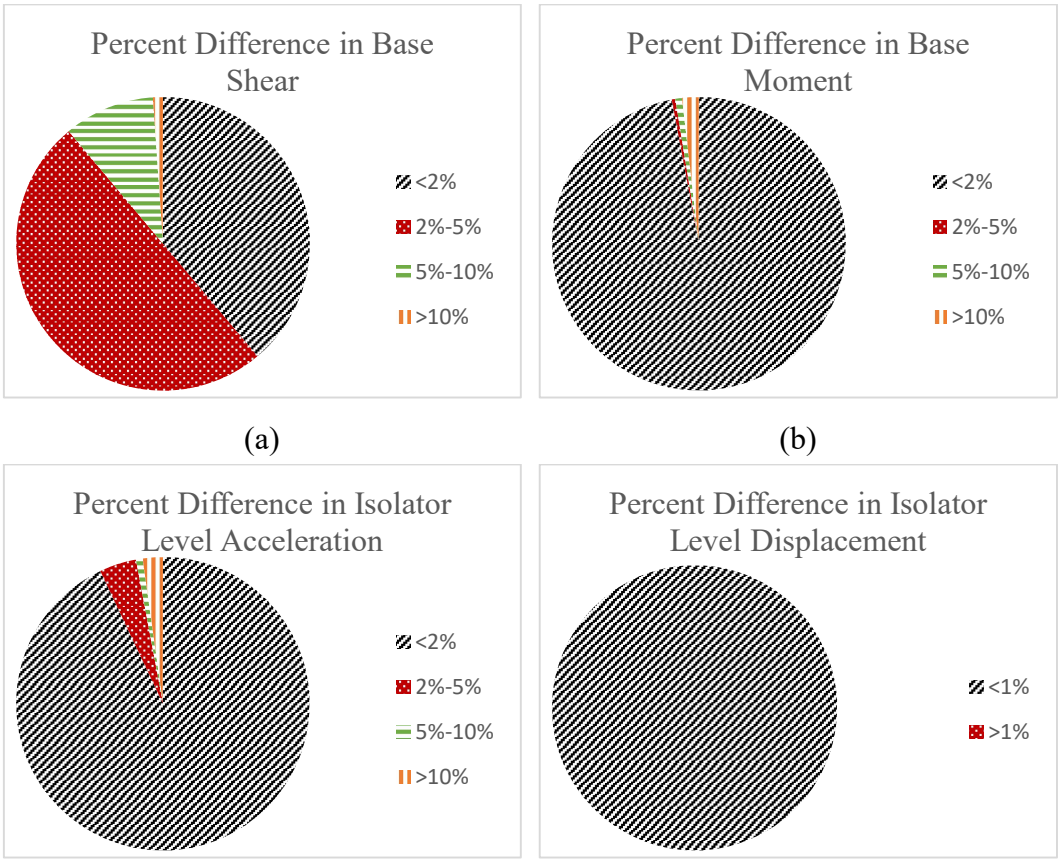

Figure 5.1. Percent Difference in Friction Isolator and Plastic-Wen Results, (a) Base Shear, (b) Base Moment, (c) Isolator L. Acceleration, (d) Isolator L. Disp.

Moreover, graphs of the ratio of Friction Isolator results to Plastic-Wen results for the S-DOF system and 2-story, 4-story, 8-story, and 12-story structures are presented in Figure 5.2. For S-DOF analysis, the mass of the 2-story building is taken as the mass of the S-DOF system. The graphs are prepared for different soil classes, and the benchmark properties are used as the isolator properties. As observed from the graphs, isolator level displacement results are the same for Friction Isolator and

Plastic-Wen. However, as the number of stories increases, a difference up to 5% occurs in the base shear results.

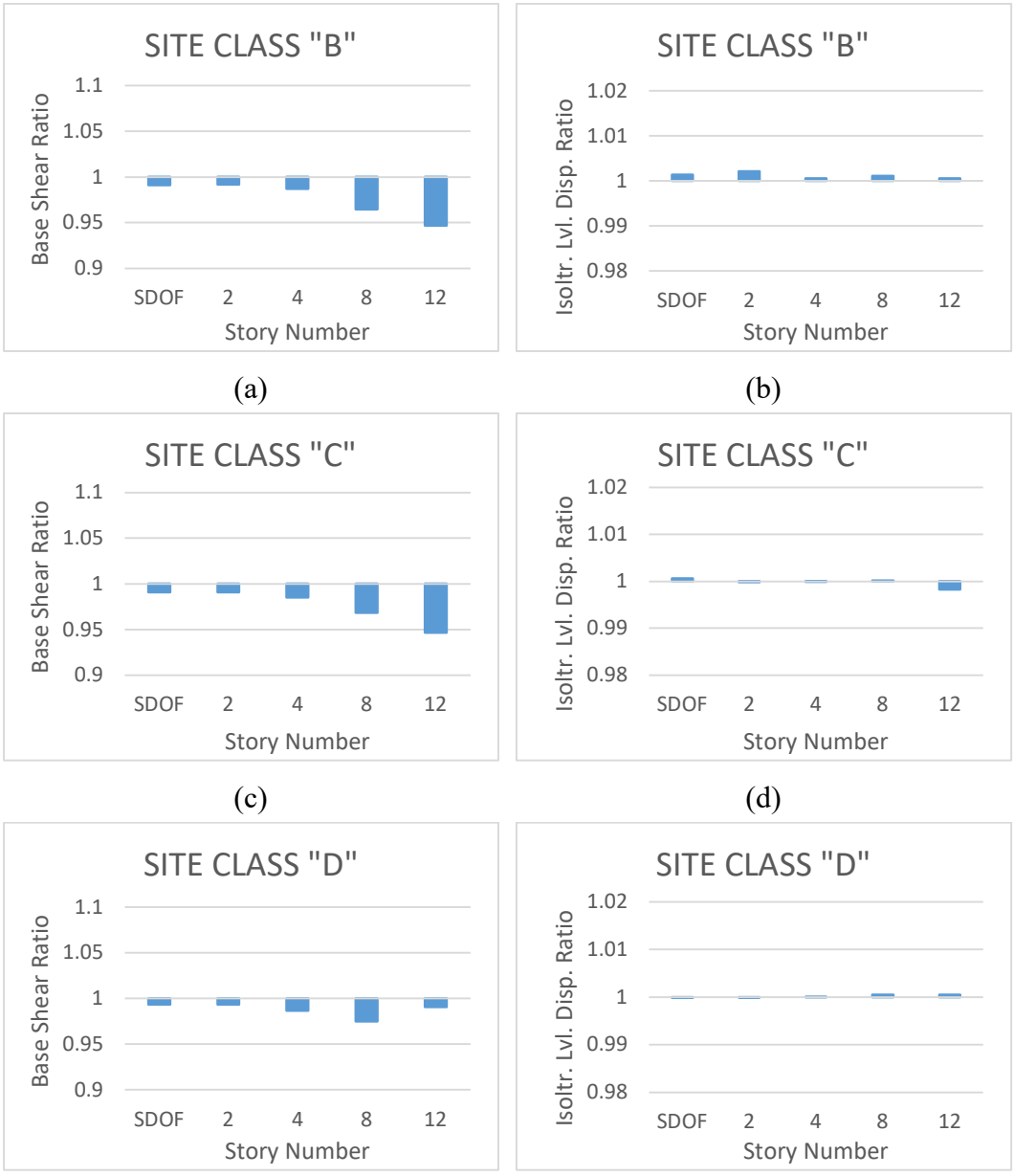

Figure 5.2. Ratio of Friction Isolator Results to Plastic-Wen Results, (a) Base Shear Ratio for Site Class B, (b) Isolator Level Displacement Ratio for Site Class B, (c) Base Shear Ratio for Site Class C, (d) Isolator Level Displacement Ratio for Site Class C, (e) Base Shear Ratio for Site Class D, (f) Isolator Level Displacement Ratio for Site Class D

5.1.2.2 Column and Beam Results

The percentage difference graphs for the column axial load, column moment, and beam moment results are presented in Figure 5.4, Figure 5.5, Figure 5.6, respectively. The selection of interior and exterior columns and beams on the first story, mid-story, and the top story is shown in Figure 5.3. The total area represents 270 analysis models for all charts, except for mid-story element force results. Since it is not possible to obtain results for mid-story elements for 2-story buildings, the total area represents 235 analysis models for these cases.

The results are obtained by excluding the loads caused by the dead load of the building. In other words, only the loads directly caused by the earthquake forces are compared. Since the difference is less than 2% in most of the cases, the results are found to be highly consistent. The most inconsistent results are obtained from the top stories and outer elements for all results, except column axial load results. It is observed that the axial load results of inner columns are more inconsistent than the outer columns.

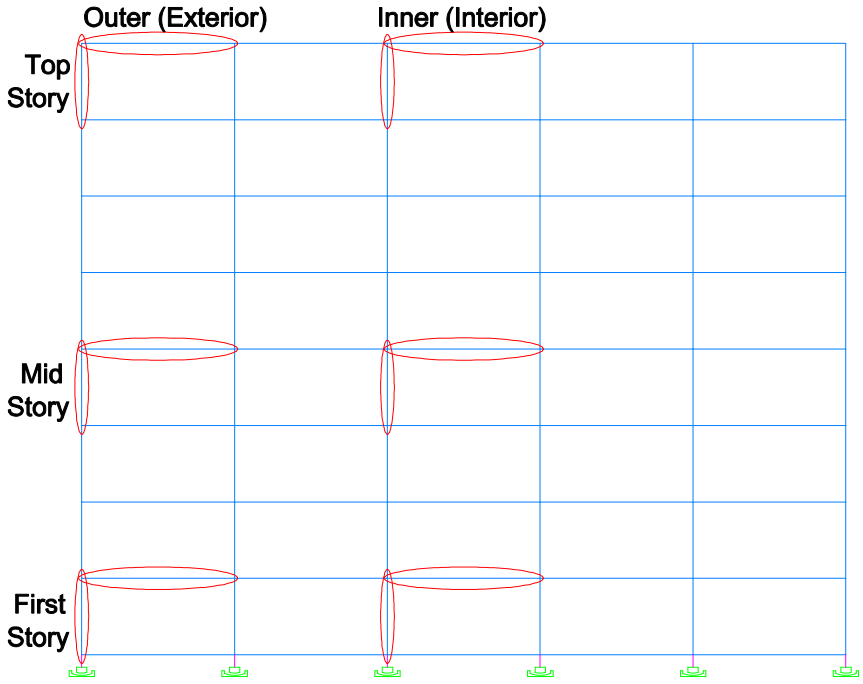

Figure 5.3. Selection of Columns and Beams to be Examined

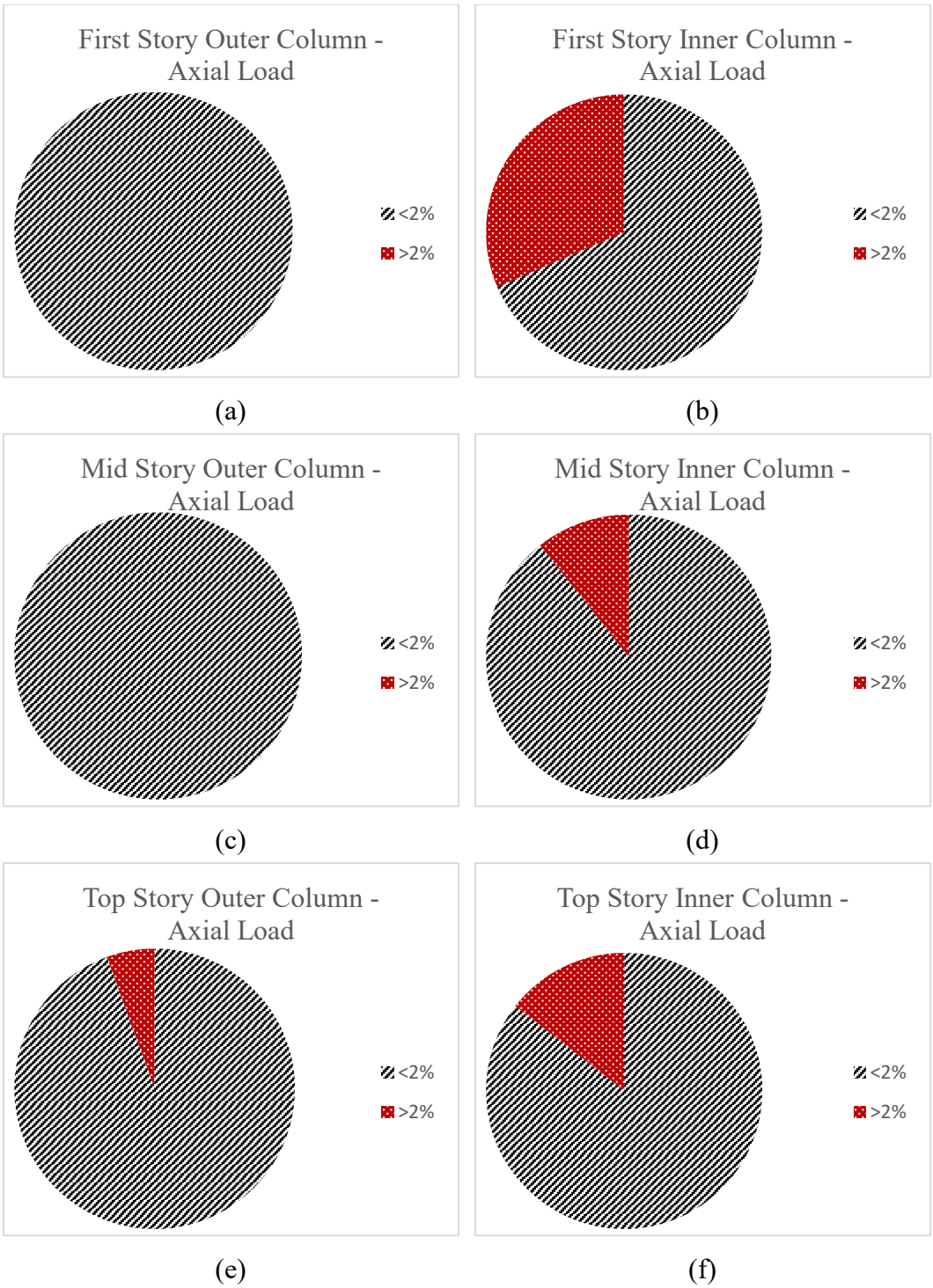

Figure 5.4. Percent Difference in Friction Isolator and Plastic-Wen Column Axial Load Results, (a) First Story Outer Column, (b) First Story Inner Column, (c) Mid-Story Outer Column, (d) Mid-Story Inner Column, (e) Top Story Outer Column, (f) Top Story Inner Column

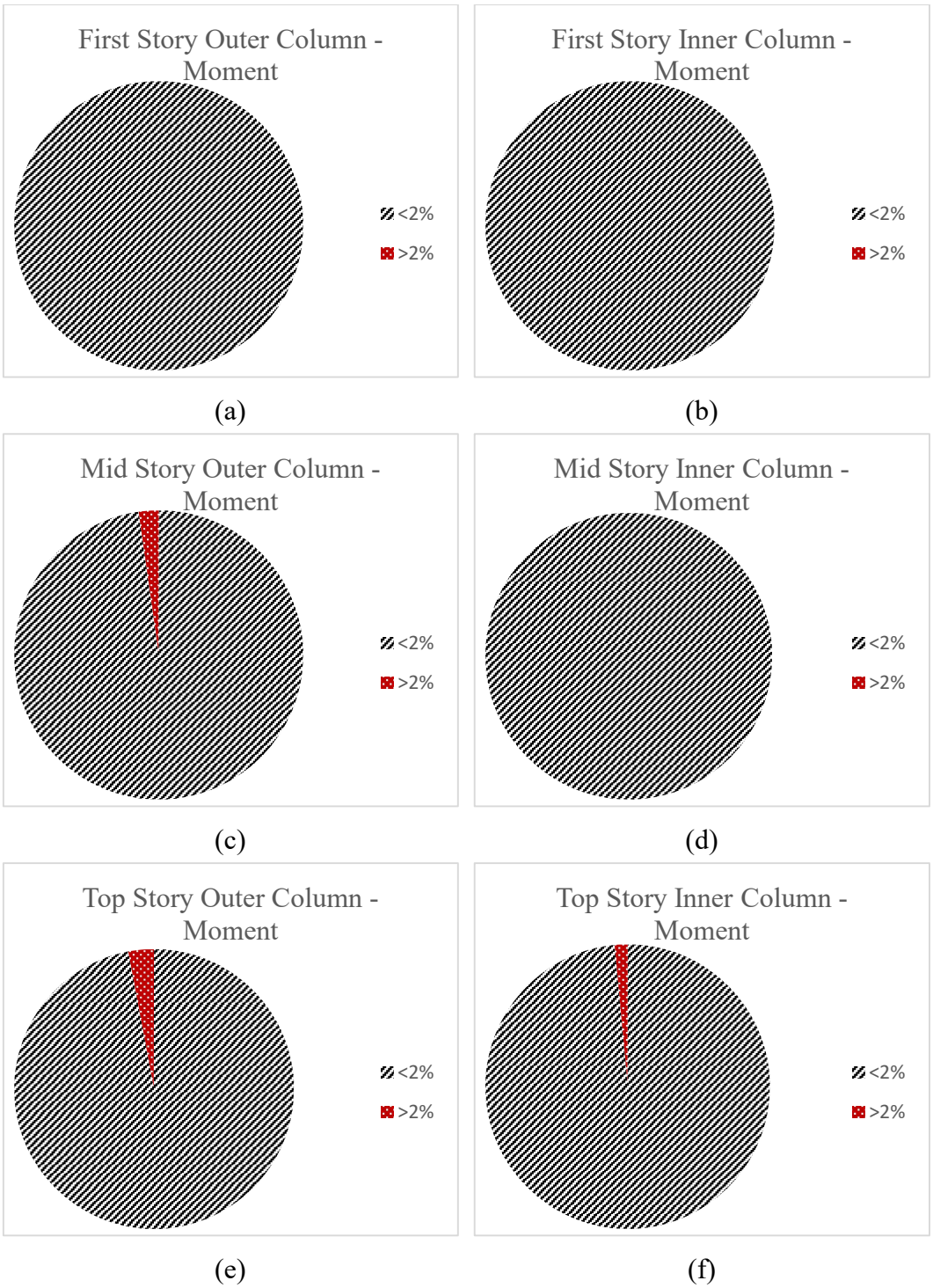

Figure 5.5. Percent Difference in Friction Isolator and Plastic-Wen Column Moment Results, (a) First Story Outer Column, (b) First Story Inner Column, (c) Mid-Story Outer Column, (d) Mid-Story Inner Column, (e) Top Story Outer Column, (f) Top Story Inner Column

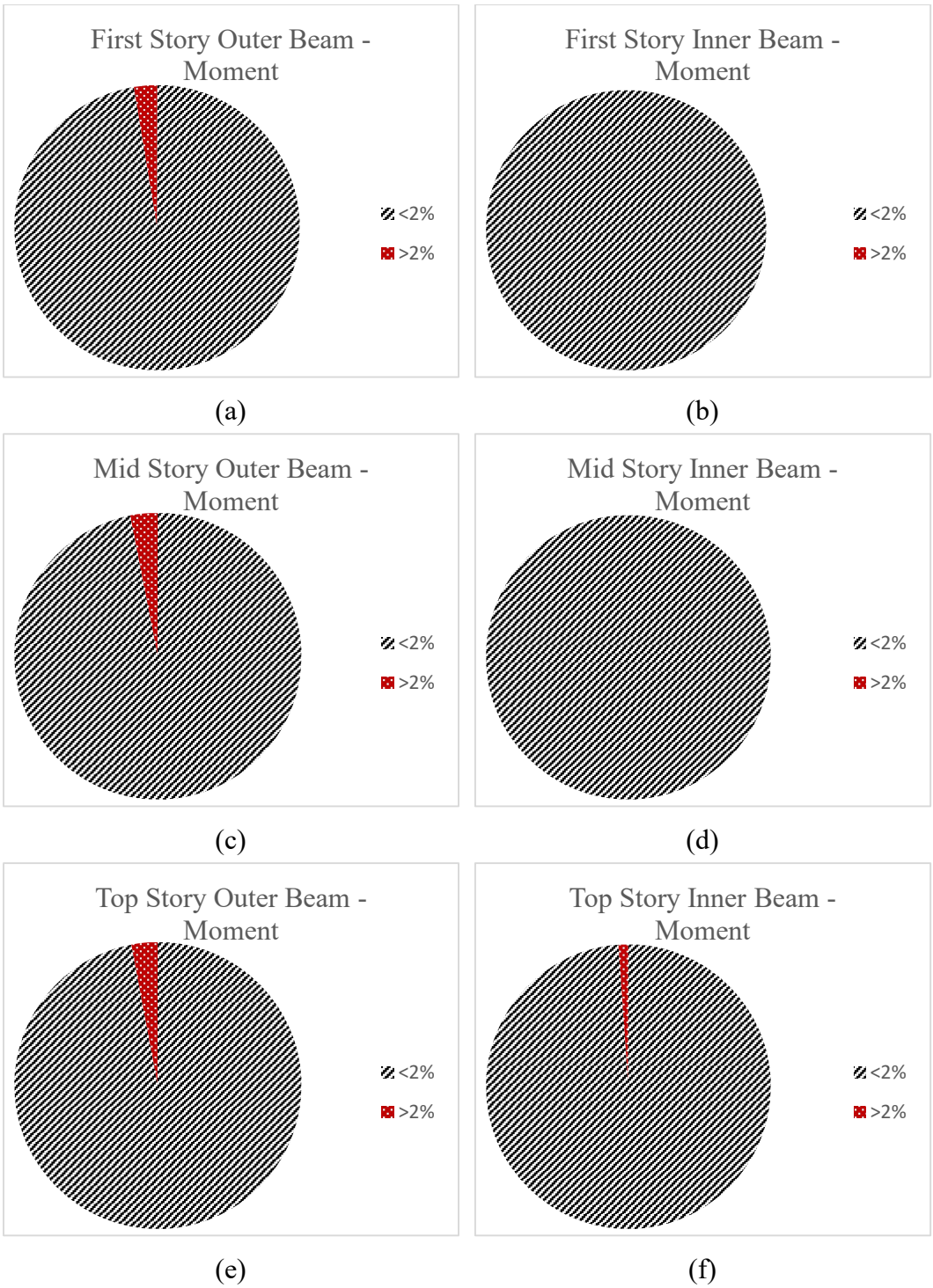

Figure 5.6. Percent Difference in Friction Isolator and Plastic-Wen Beam Moment Results, (a) First Story Outer Column, (b) First Story Inner Column, (c) Mid-Story Outer Column, (d) Mid-Story Inner Column, (e) Top Story Outer Column, (f) Top Story Inner Column

5.2 Effect of Limiting Equivalent Damping Coefficient

As mentioned in Chapter 4, the equivalent damping coefficient is limited between 5% and 30% in the iterative procedure of the equivalent linear method. According to the equivalent linear analysis results, the equivalent damping coefficient of 157 analysis models out of 270 is limited to 30%, and none of these models are limited to 5%. In this section, analysis models subjected to the limitation of the equivalent damping coefficient will be examined, and these models will be analyzed without limitation, and the effect of the limitation on the results will be examined. The number of cases with better estimation according to the base shear, base moment, isolator level acceleration, and displacement results are presented in Figure 5.7.

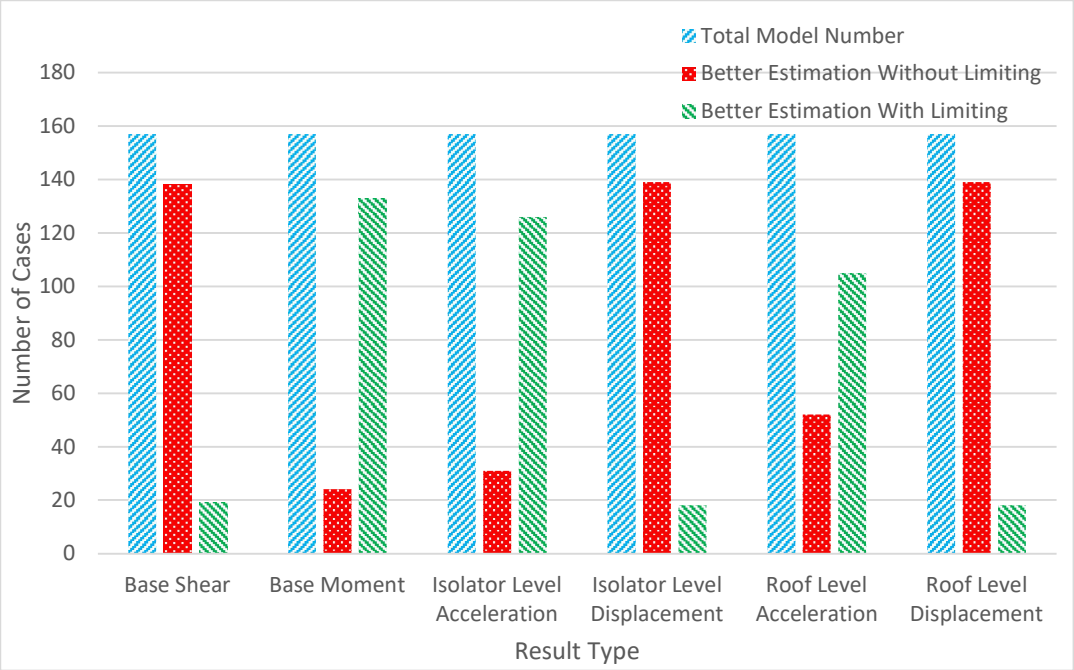

Figure 5.7. Number of Cases With Better Estimated Results According to The Limitation of The Equivalent Linear Damping Coefficient

According to the base shear, isolator level, and roof level displacement results, if the equivalent damping coefficient is not limited, more than 138 analysis models out of 157 resulted in better estimation of the equivalent linear method. On the other hand, in most cases where the equivalent damping coefficient is limited, the equivalent linear method estimated better base moment, isolator level, and roof level acceleration results.

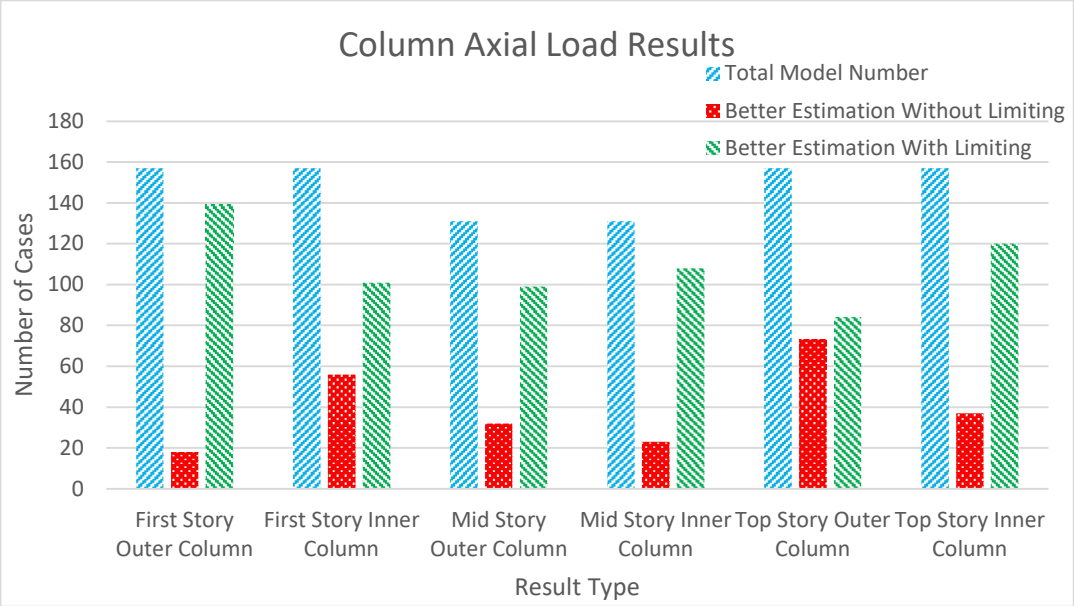

Figure 5.8. Number of Cases With Better-Estimated Column Axial Load Results According to The Limitation of The Equivalent Linear Damping Coefficient

The number of cases with better-estimated column axial load, column moment, and beam moment results according to the limitation of the equivalent linear damping coefficient are presented in Figure 5.8, Figure 5.9, and Figure 5.10, respectively. As observed from these figures, all element results are better estimated when the equivalent linear damping coefficient is limited. For this reason, limiting the equivalent damping coefficient between 5% and 30% will lead to better estimation for most of the analysis results.

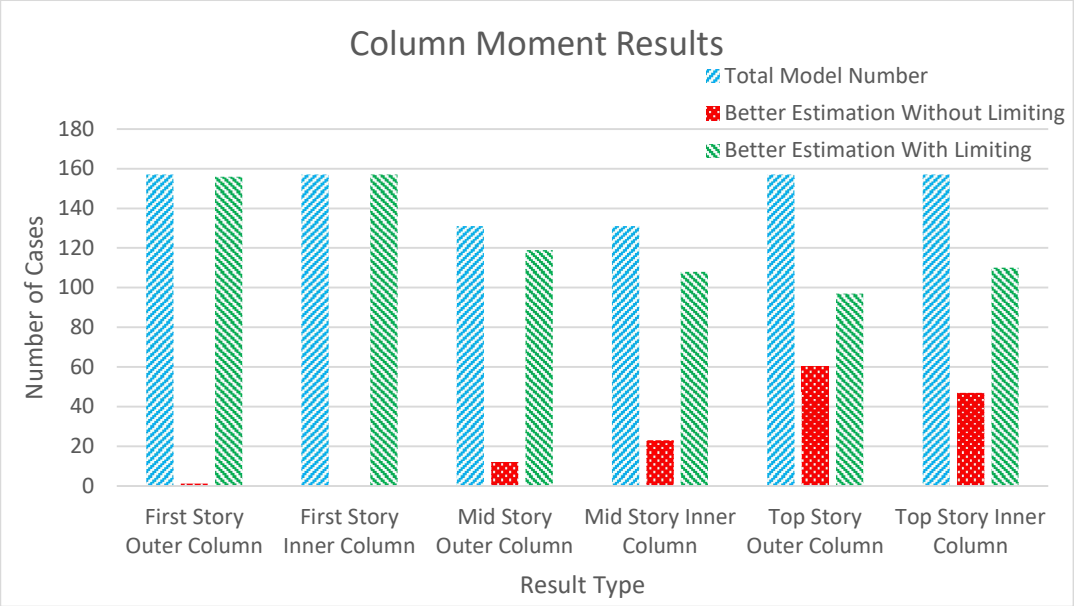

Figure 5.9. Number of Cases With Better-Estimated Column Moment Results According to The Limitation of The Equivalent Linear Damping Coefficient

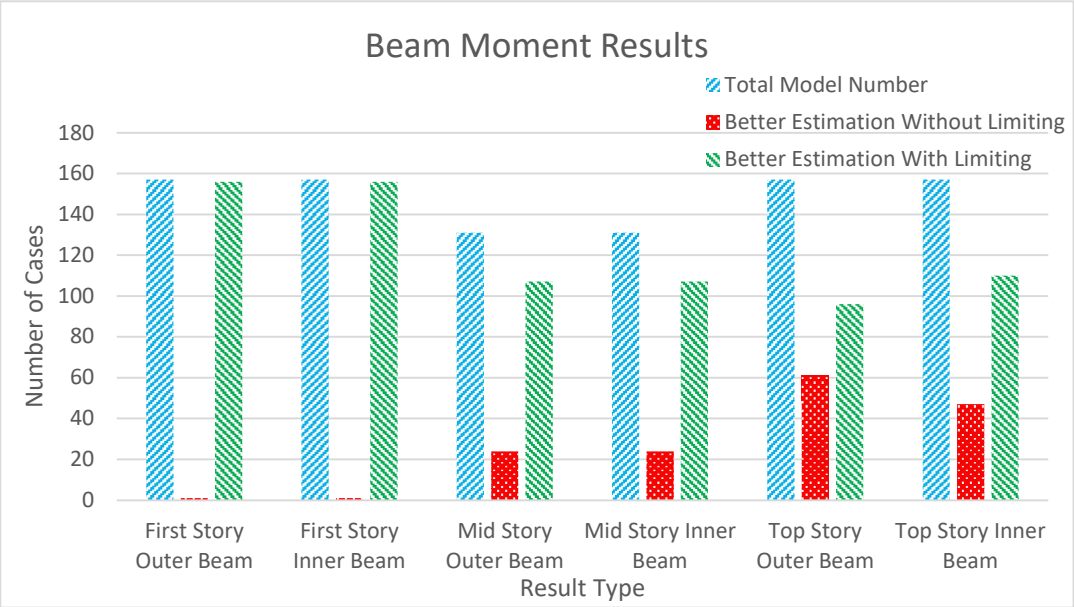

Figure 5.10. Number of Cases With Better-Estimated Beam Moment Results According to The Limitation of The Equivalent Linear Damping Coefficient

CHAPTER 6

PARAMETRIC EVALUATION OF THE S-DOF SYSTEM

6.1 Introduction

In this chapter, the base shear, acceleration and displacement results of S-DOF analysis will be presented, and the effect of the selected parameters will be evaluated and discussed. Benchmark results are presented for 8-story and 5-bay structures with isolator parameters of $\mu = 0.5$ and R=5m and soil site class C. The total weight of the corresponding M-DOF structure is used for the buildings with different story and bay numbers.

6.2 Evaluation of the Results

6.2.1 Base Shear

The base shear is an indicator of the consistency of the earthquake force transferred to the superstructure. The base shear results of the two methods and their ratio are presented in Figure 6.1 and Figure 6.2, respectively.

As observed from the graphs, base shear is overestimated up to 20% by the equivalent linear method. The difference between the results increases as the average shear wave velocity and radius of curvature decrease and the peak ground acceleration, story number, and bay number increase. However, the accuracy of equivalent linear method increases as the radius of curvature increases. Other selected parameters has no significant or conclusive effect on the base shear results.

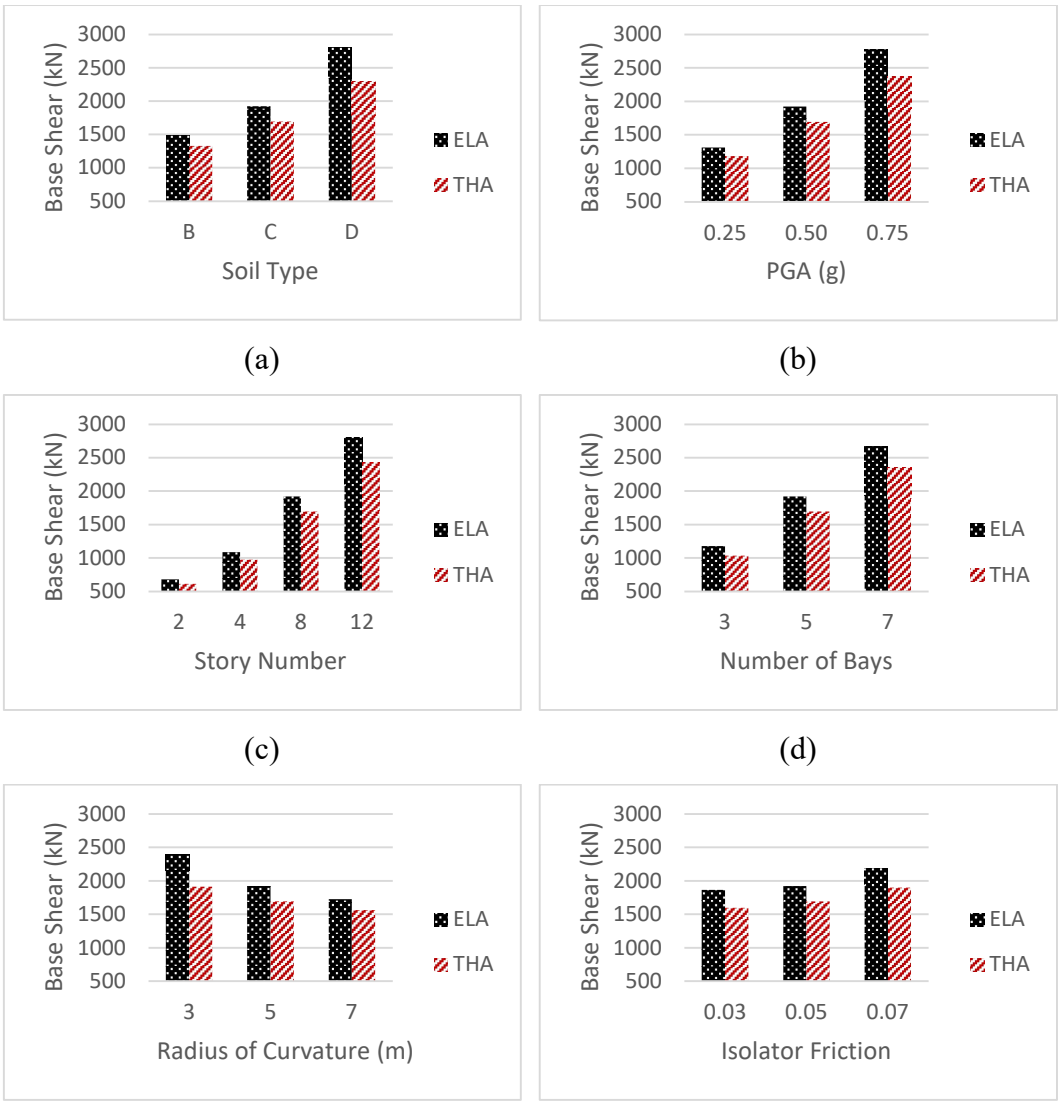

Figure 6.1. Effect of Selected Parameters on Base Shear Results for S-DOF Structure With Benchmark Properties, (a) Soil Type, (b) Peak Ground Acceleration, (c) Story Number, (d) Number of Bays, (e) Radius of Curvature, (f) Isolator Friction

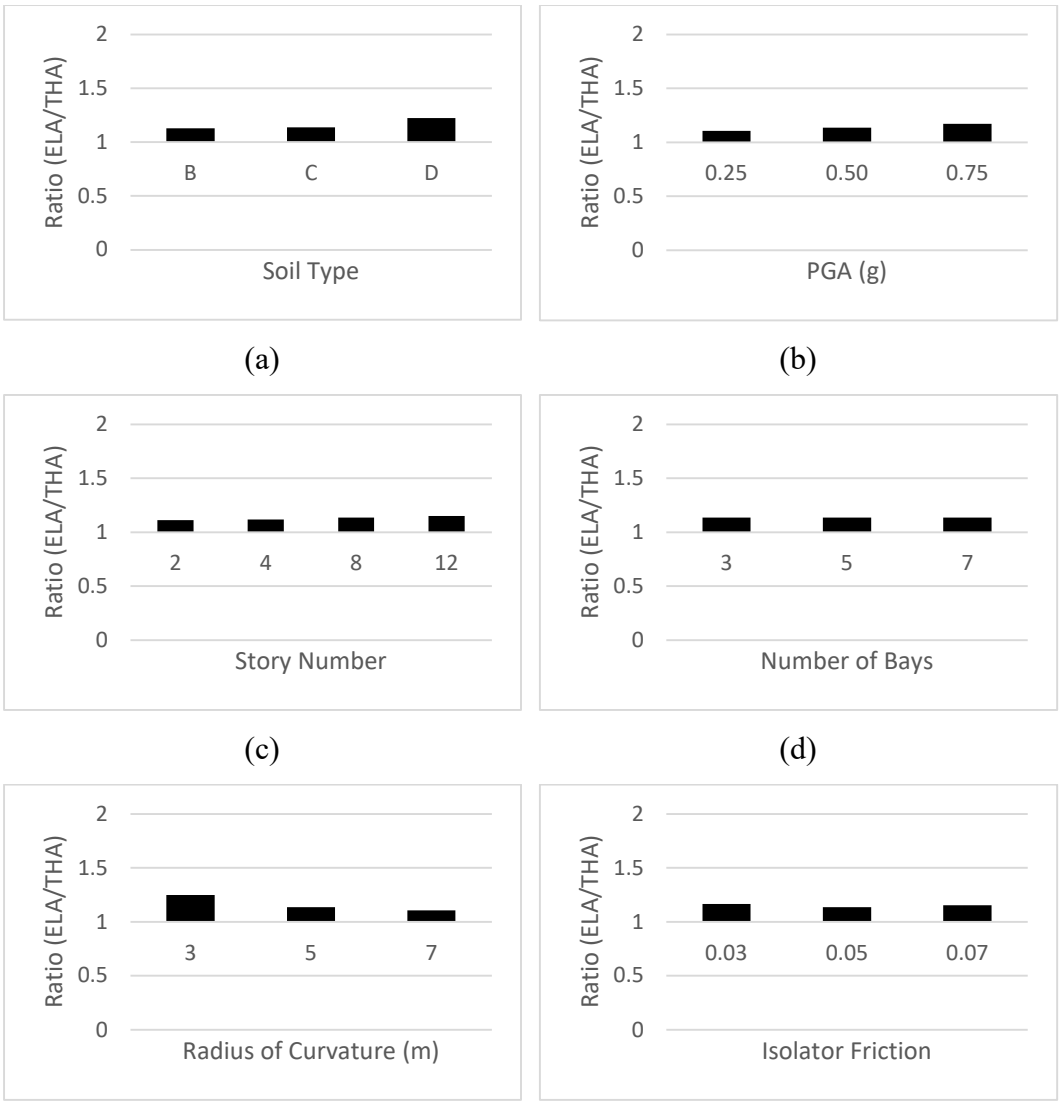

Figure 6.2. Ratio of ELA Base Shear Results to THA Base Shear Results of S-DOF Structure With Benchmark Properties, (a) Soil Type, (b) Peak Ground Acceleration, (c) Story Number, (d) Number of Bays, (e) Radius of Curvature, (f) Isolator Friction

6.3 Displacement

As described in Chapter 4, the iterative procedure of the equivalent linear method is based on the displacement as it directly affects the equivalent stiffness of the isolation system. Hence, the accuracy of the displacement is one of the most important criteria when evaluating the accuracy of the equivalent linear method. The displacement results and the ratio of the equivalent linear method results to the nonlinear method results are presented in Figure 6.3 and Figure 6.4, respectively.

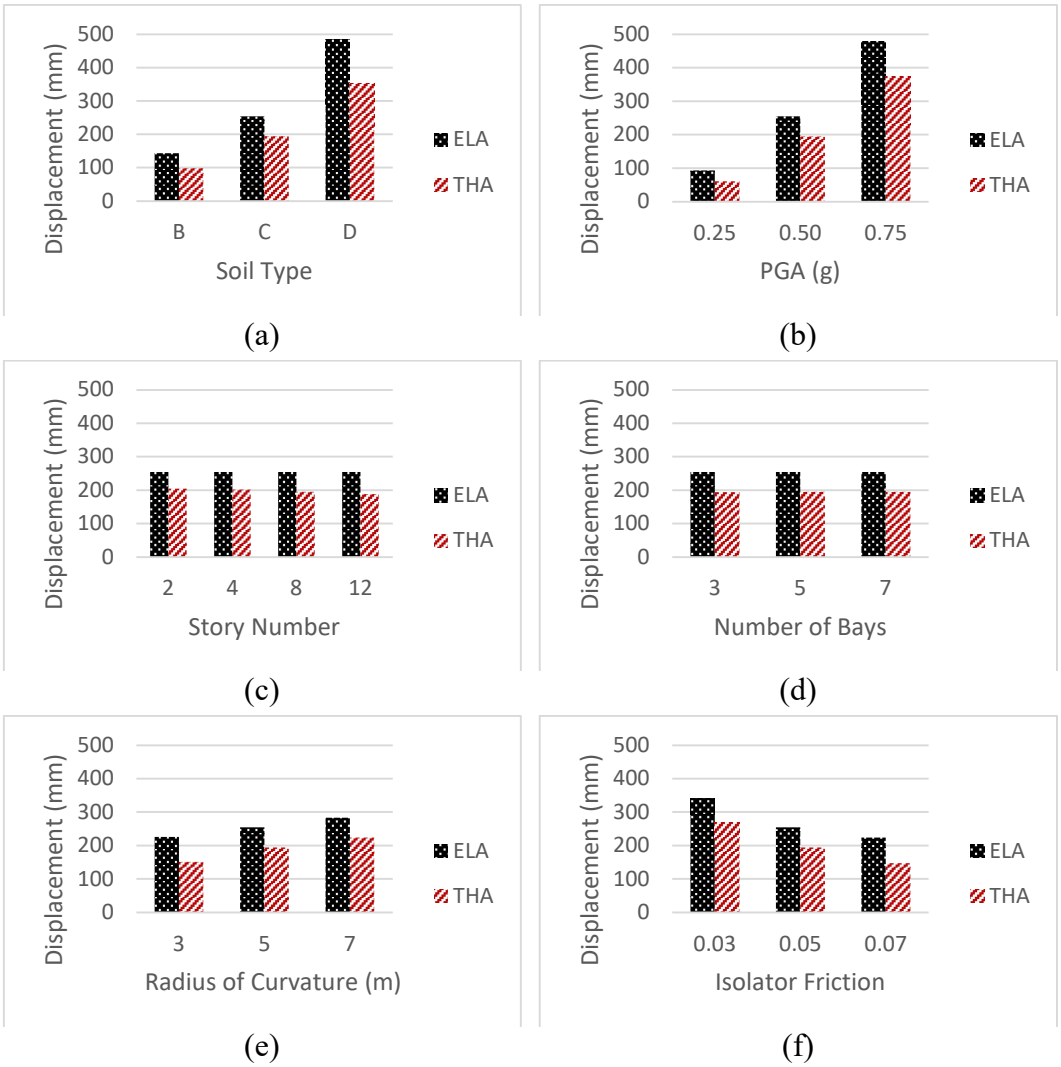

Figure 6.3. Effect of Selected Parameters on the Displacement Results for S-DOF Structure With Benchmark Properties, (a) Soil Type, (b) Peak Ground Acceleration, (c) Story Number, (d) Number of Bays, (e) Radius of Curvature, (f) Isolator Friction

The displacements are overestimated by 20% to 50% by the equivalent linear method. As observed from the charts, the accuracy of the equivalent linear method increases as the peak ground acceleration and radius of curvature increase and the isolator friction decreases. However, the displacement results of both methods appear to be unaffected by the bay number. Similarly, while the equivalent linear analysis results do not change depending on the story number, there is a slight decrease in the nonlinear analysis results as the story number increases. In other words, there is a slight decrease in the accuracy of the equivalent linear method as the story number increases. On the other hand, there is no correlation between the soil type and the accuracy.

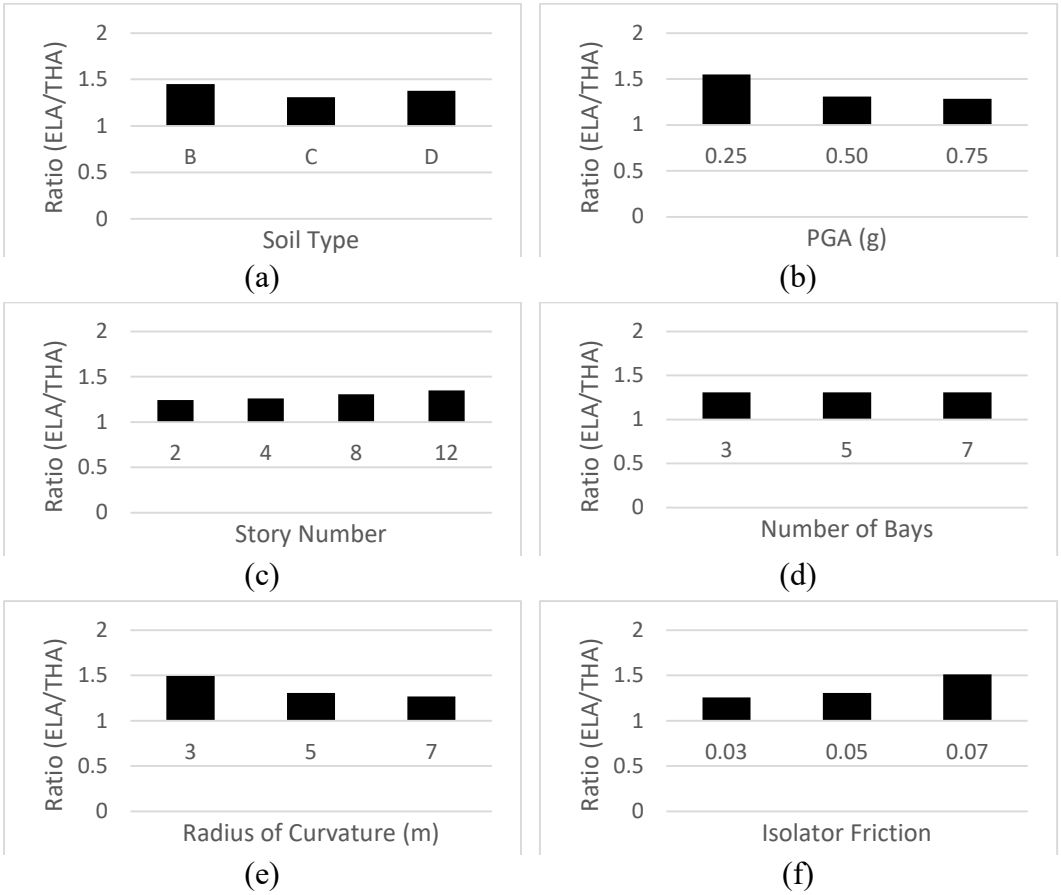

Figure 6.4. Ratio of ELA Displacement Results to THA Displacement Results of S-DOF Structure with Benchmark Properties, (a) Soil Type, (b) Peak Ground Acceleration, (c) Story Number, (d) Number of Bays, (e) Radius of Curvature, (f) Isolator Friction

6.4 Acceleration

The acceleration results and the ratio of the equivalent linear method results to the nonlinear method results are presented in Figure 6.5 and Figure 6.6, respectively.

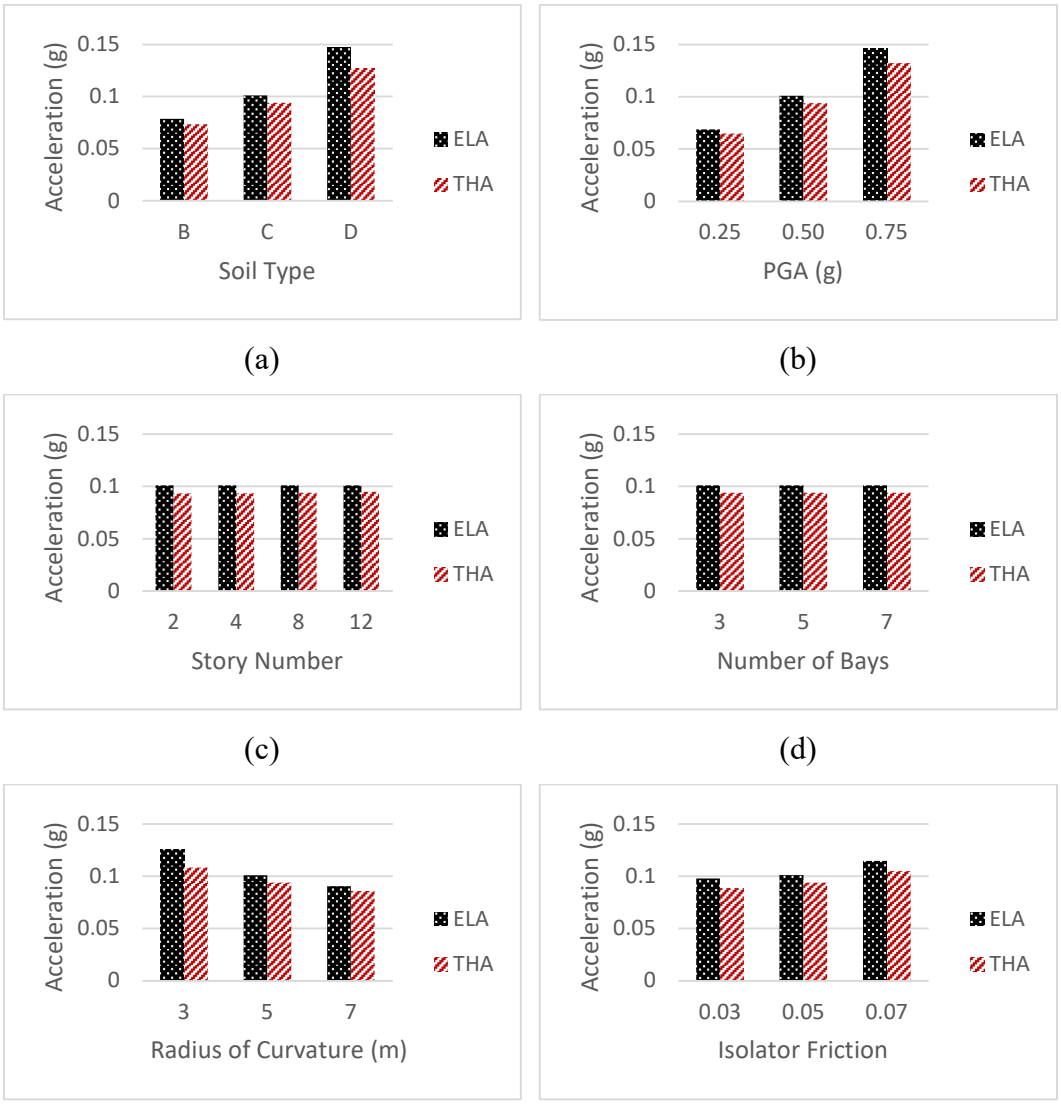

Figure 6.5. Effect of Selected Parameters on the Acceleration Results for S-DOF Structure With Benchmark Properties, (a) Soil Type, (b) Peak Ground Acceleration, (c) Story Number, (d) Number of Bays, (e) Radius of Curvature, (f) Isolator Friction

It is observed that the acceleration results of the equivalent linear method for S-DOF structures are quite accurate. The equivalent linear method overestimates the accelerations by up to 15%. However, as the peak ground acceleration, radius of curvature, and average shear wave velocity increase, the accuracy increases.

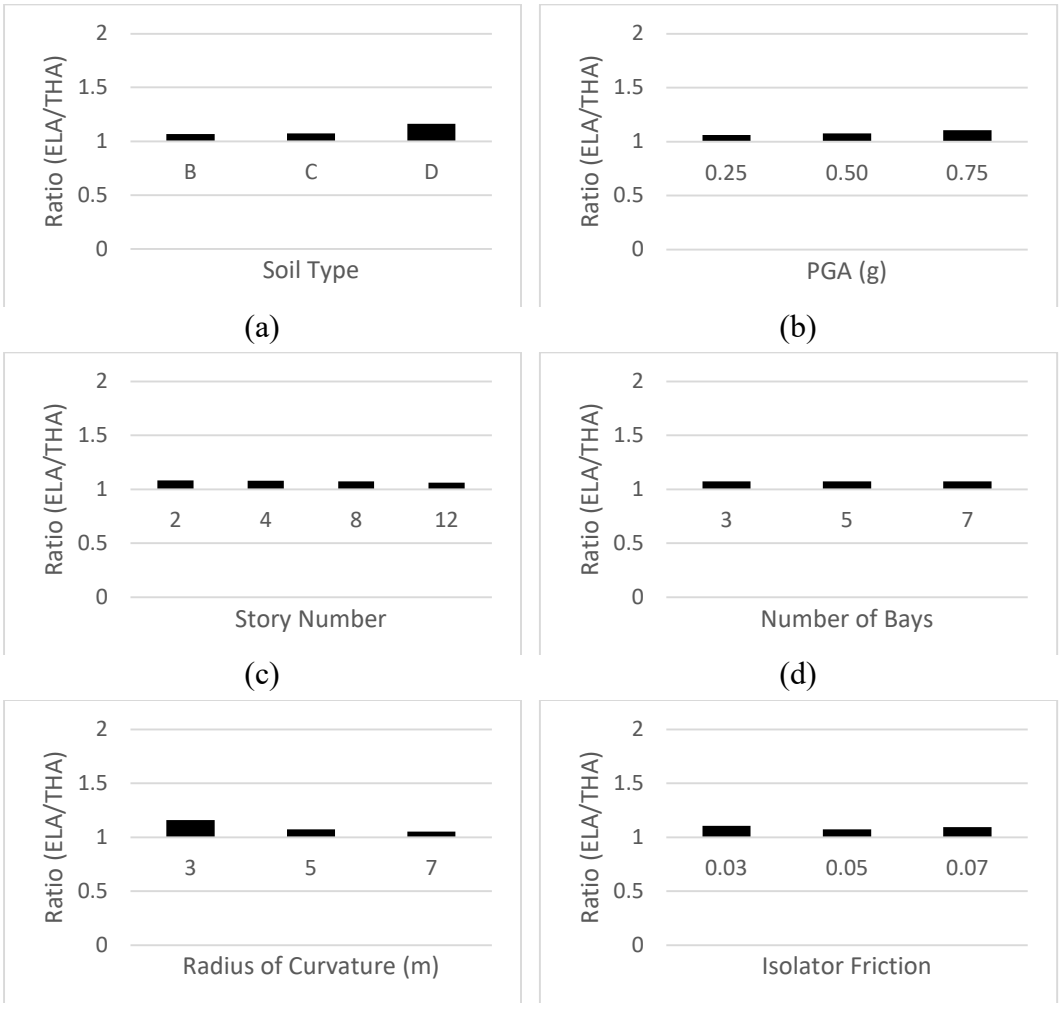

Figure 6.6. Ratio of ELA Acceleration Results to THA Acceleration Results of S-DOF Structure with Benchmark Properties, (a) Soil Type, (b) Peak Ground Acceleration, (c) Story Number, (d) Number of Bays, (e) Radius of Curvature, (f) Isolator Friction

CHAPTER 7

PARAMETRIC EVALUATION OF THE RESULTS

7.1 Introduction

In this chapter, the results of the M-DOF system are presented, and the effects of the selected parameters are evaluated and discussed. Firstly base shear and base moment results of the equivalent linear analysis and time history analysis are compared. Then the acceleration results, displacement results, maximum inter-story drift ratio results, and forces in columns and beams are presented. Benchmark results are presented for 8-story and 5-bay structures with isolator parameters of $\mu = 0.5$ and R=5m and soil site class C.

7.2 Evaluation of the Results

7.2.1 Base Shear and Base Moment Results

Base shear and base moment of the structure is also an indication of the consistency of earthquake forces that transferred to the superstructure. The results of equivalent linear analysis and time history analysis are presented in the same graph, and 6 different graphs are prepared in order to evaluate the effect of parameters. Base shear results for the two methods and their ratio are presented in Figure 7.1 and Figure 7.2, respectively.

As observed from the graphs, base shear is overestimated up to 20% by the equivalent analysis. The difference between the results increases as the average shear wave velocity and radius of curvature decrease, but peak ground acceleration, story, and bay number increase. However, the accuracy of ELA increases as radius of curvature increases. Other selected parameters have no significant or conclusive

effect on the base shear results. In addition, the base shear results of both methods are nearly the same with the corresponding S-DOF results.

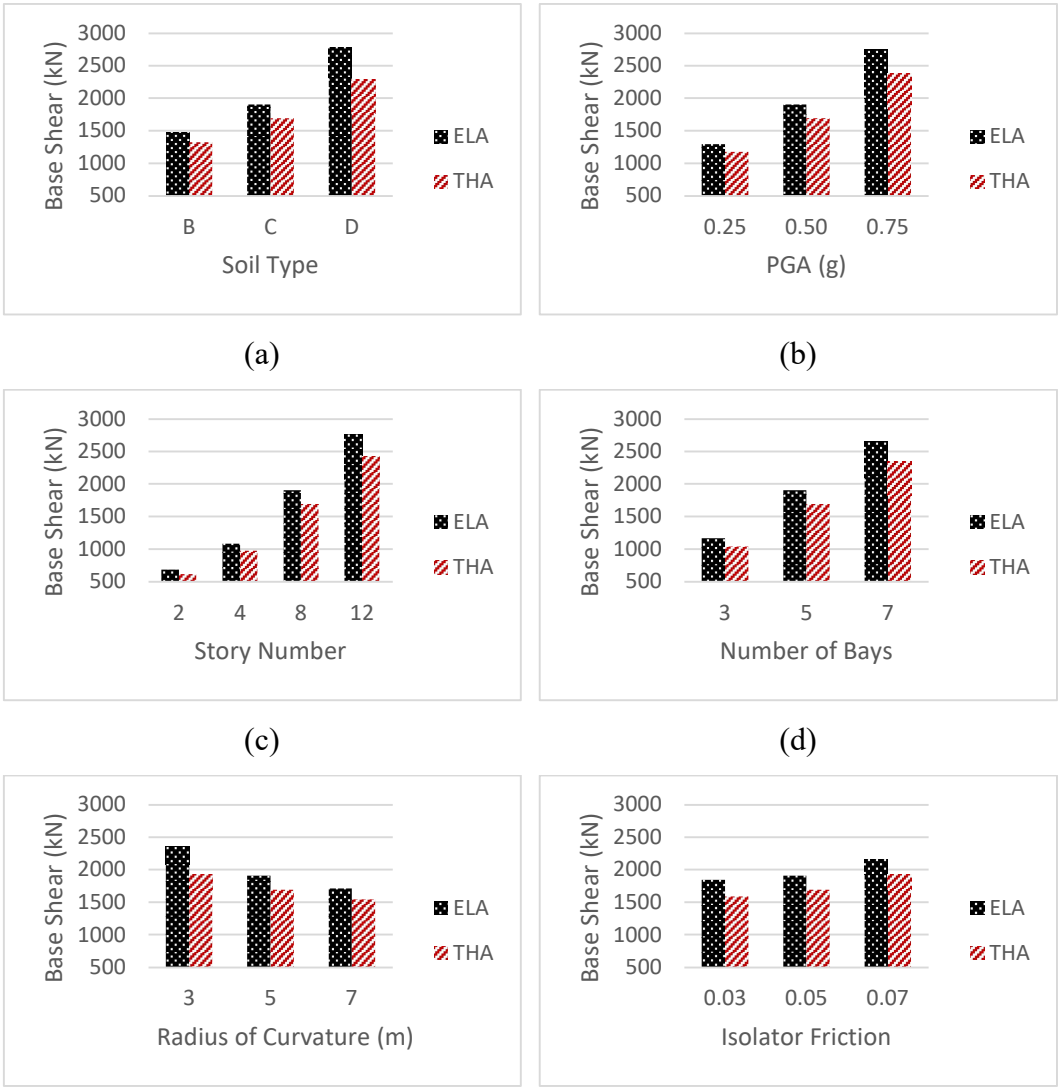

Figure 7.1. Effect of Selected Parameters on Base Shear Results for M-DOF Structure with Benchmark Properties, (a) Soil Type, (b) Peak Ground Acceleration, (c) Story Number, (d) Number of Bays, (e) Radius of Curvature, (f) Isolator Friction

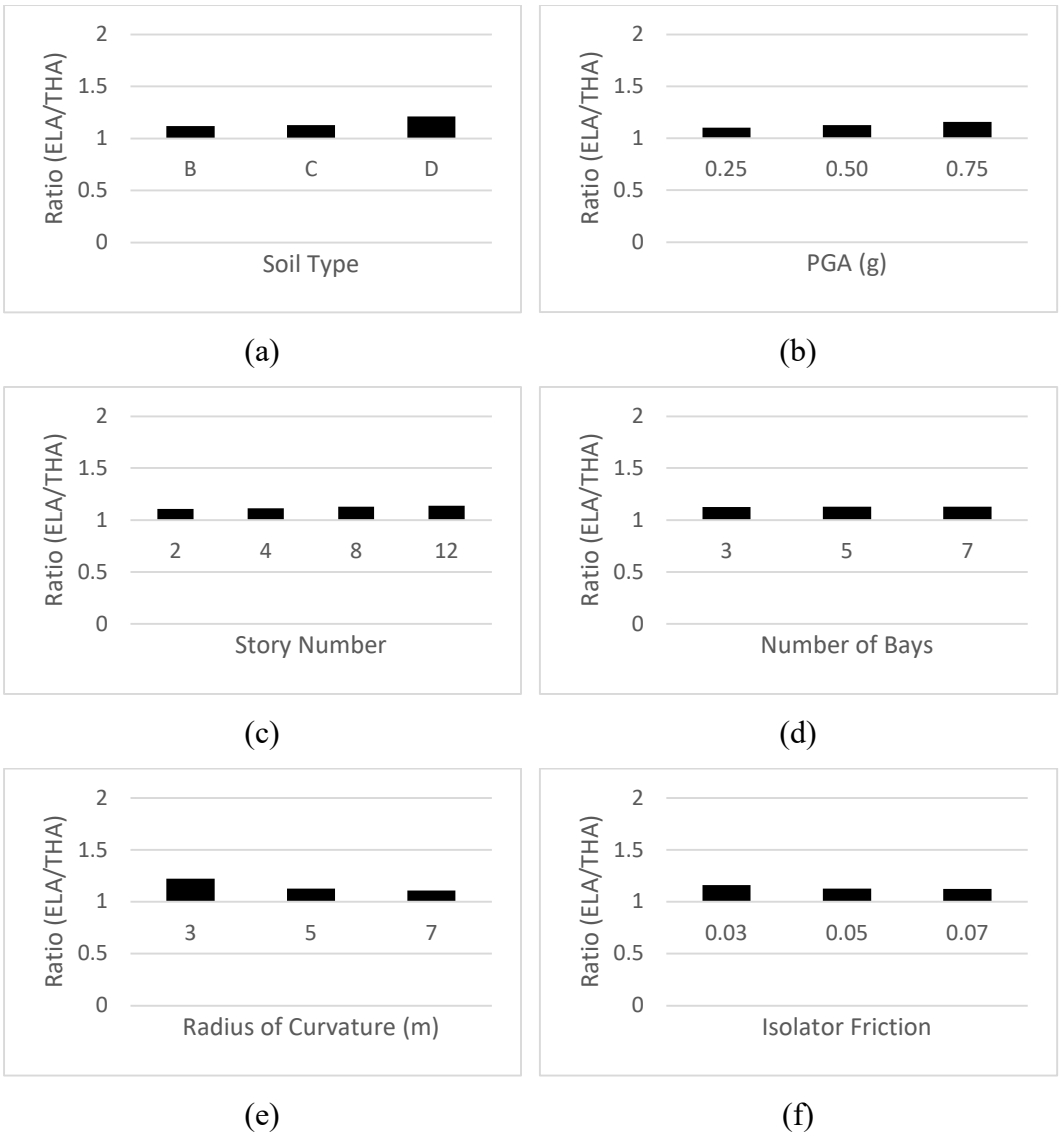

Figure 7.2. Ratio of ELA Base Shear Results to THA Base Shear Results of M-DOF Structure with Benchmark Properties, (a) Soil Type, (b) Peak Ground Acceleration, (c) Story Number, (d) Number of Bays, (e) Radius of Curvature, (f) Isolator Friction

Base moment results for the two methods and their ratio are presented in Figure 7.3 and Figure 7.4, respectively. The results of equivalent linear method and nonlinear method are highly consistent. As observed from the graphs, all analysis parameters except isolator friction, story number and bay number have almost no effect on base moment. On average, base moment results of 8-story buildings are underestimated

by 3% by the equivalent linear method. However, this difference increases to 5% for 12-story buildings, and the two method estimates the same base moments for 2-story buildings.

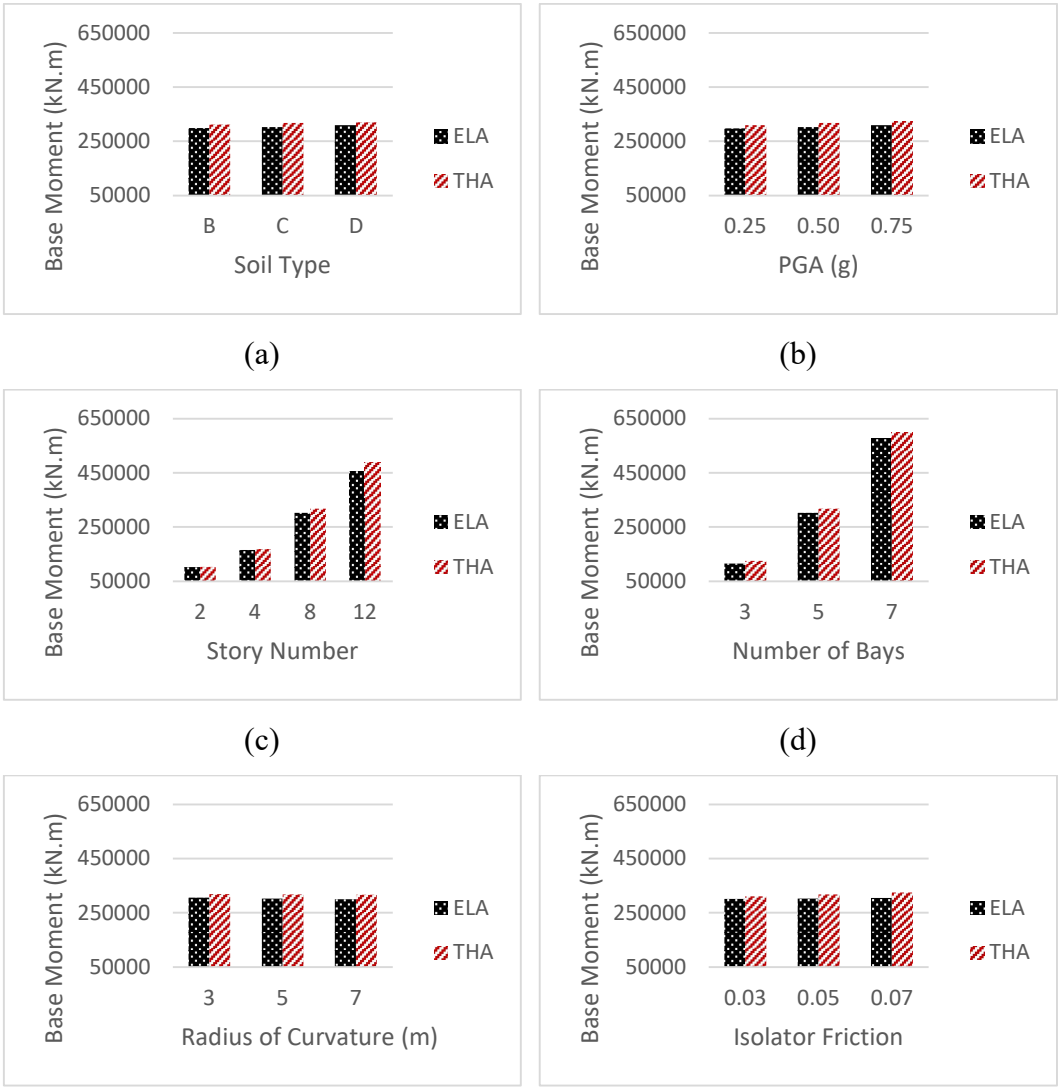

Figure 7.3. Effect of Selected Parameters on Base Moment Results for Benchmark Properties, (a) Soil Type, (b) Peak Ground Acceleration, (c) Story Number, (d) Number of Bays, (e) Radius of Curvature, (f) Isolator Friction

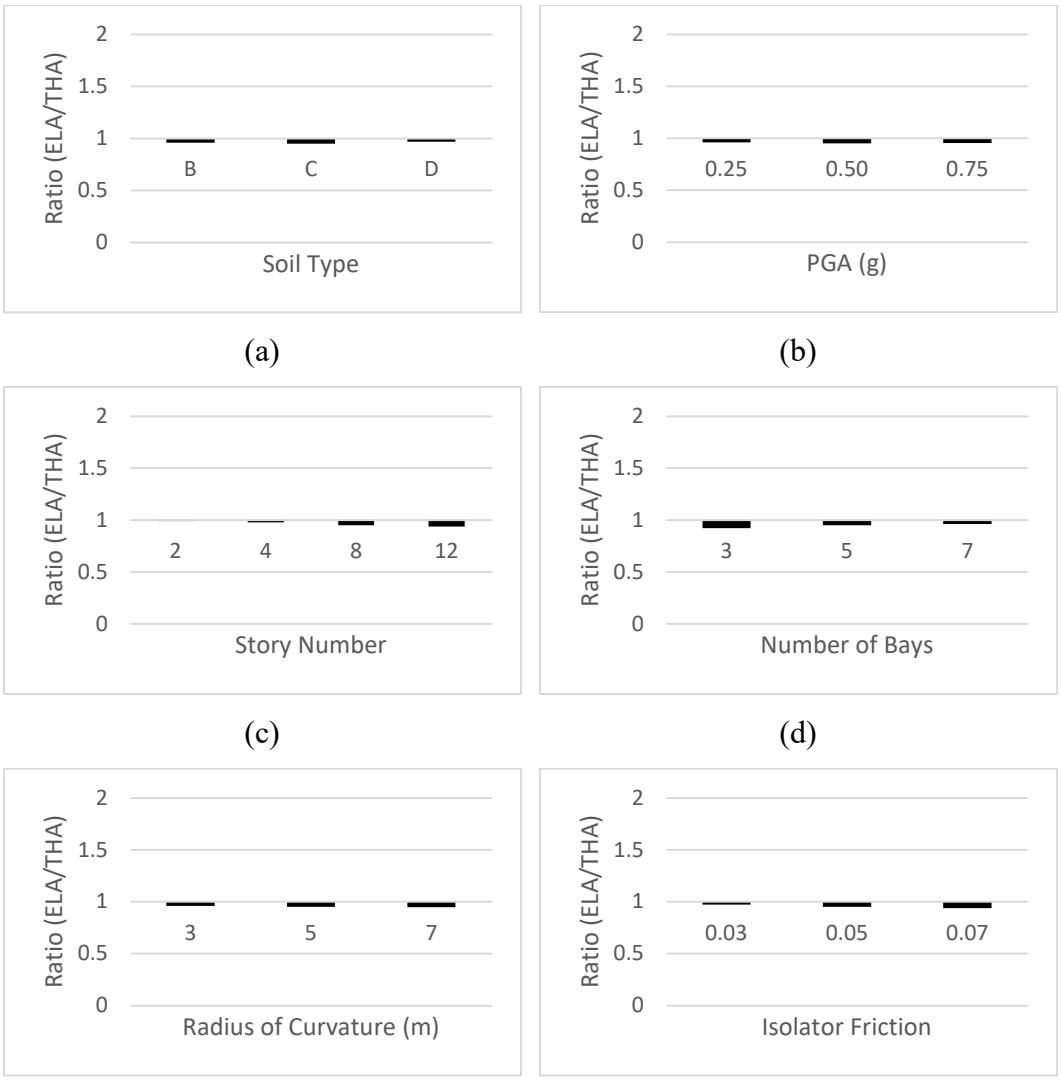

Figure 7.4. Ratio of ELA Base Moment Results to THA Base Moment Results of M-DOF Structure with Benchmark Properties, (a) Soil Type, (b) Peak Ground Acceleration, (c) Story Number, (d) Number of Bays, (e) Radius of Curvature, (f) Isolator Friction

7.2.2 Displacement Results

7.2.2.1 Isolator Level Displacements

Since the iterative procedure is based on the isolator level displacement, the accuracy of the isolator level displacement is one of the most important criteria when evaluating the accuracy of the equivalent linear analysis. The isolator level displacement results and the ratio of the equivalent linear results to the nonlinear analysis are presented in Figure 7.5 and Figure 7.6, respectively.

Firstly, the isolator level displacement results of each analysis method are exactly equal to the S-DOF displacement results of the same method. However, isolator level displacements are overestimated by 20% to 50% by equivalent linear analysis. As observed from the charts, the accuracy of the equivalent linear analysis increases as the peak ground acceleration increases. However, there is no correlation between the soil type and the accuracy.

On the other hand, the accuracy of the equivalent linear method increases as the radius of curvature increases and isolator friction decreases. However, the displacement results of both methods appear to be unaffected by the bay number. Similarly, while the equivalent linear analysis results do not change depending on the story number, there is a slight decrease in the nonlinear analysis results as the story number increase. This leads to a slight decrease in the accuracy of the equivalent linear analysis as the story number increase.

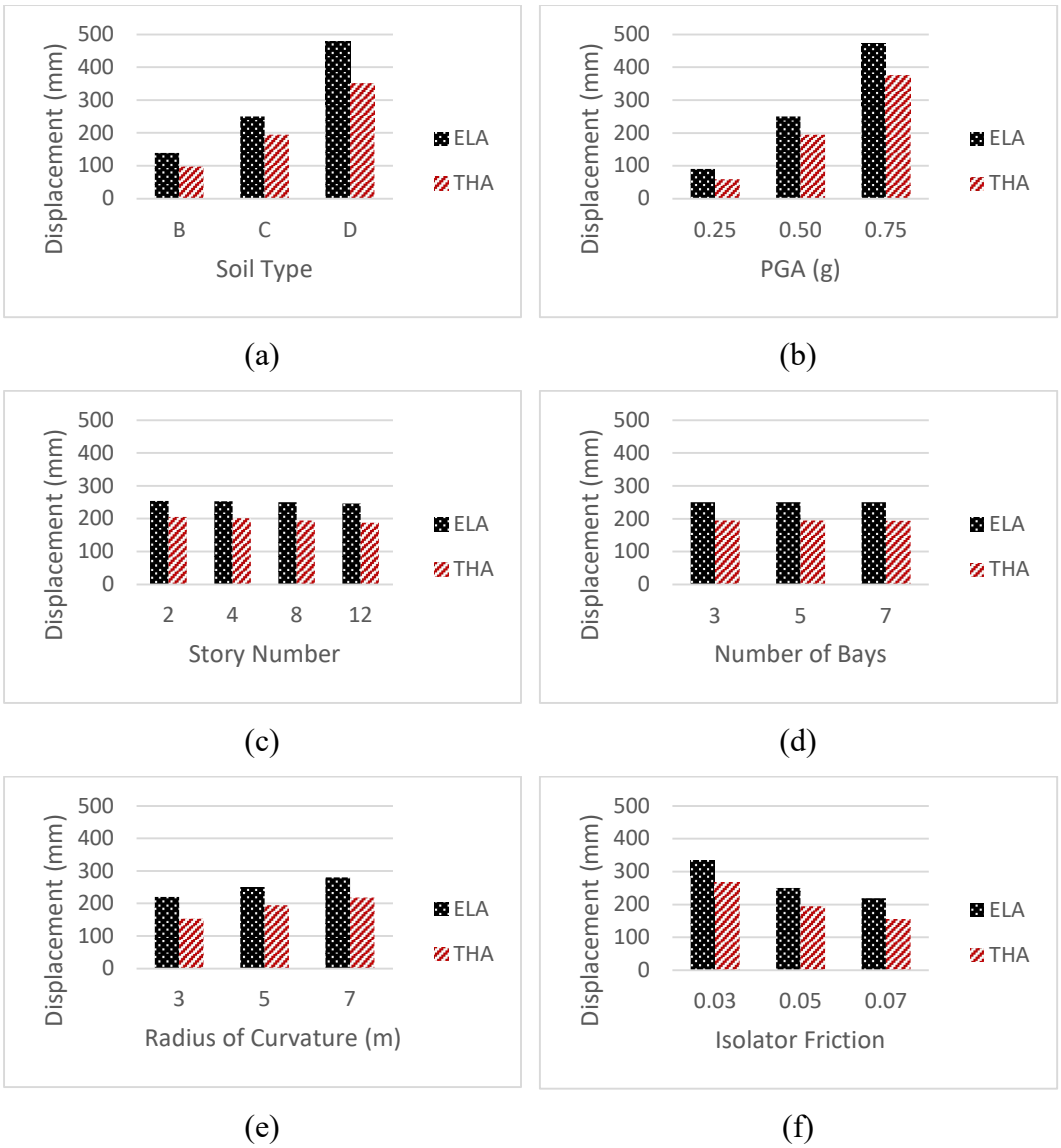

Figure 7.5. Effect of Selected Parameters on the Isolator Level Displacement Results for Benchmark Properties, (a) Soil Type, (b) Peak Ground Acceleration, (c) Story Number, (d) Number of Bays, (e) Radius of Curvature, (f) Isolator Friction

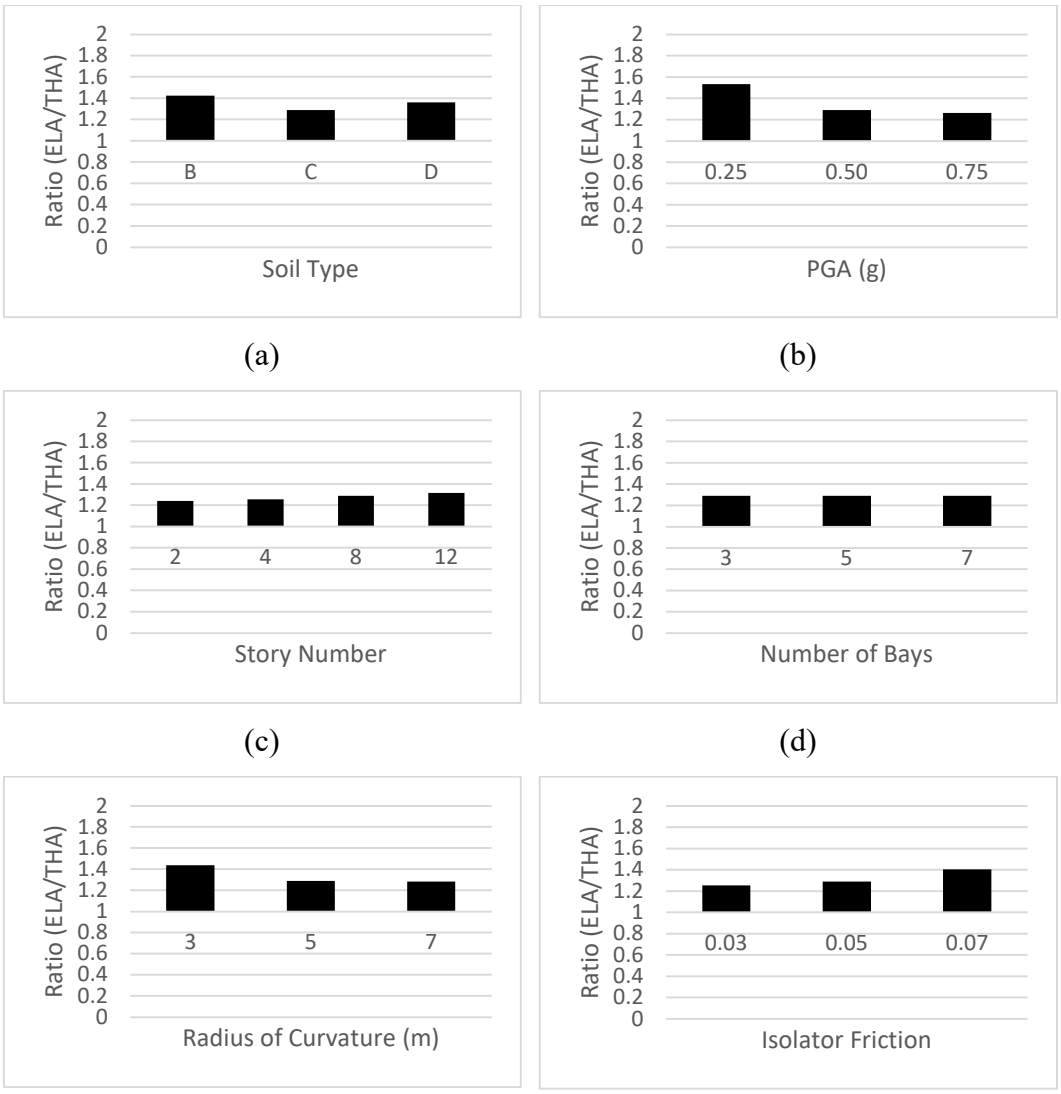

Figure 7.6. Ratio of ELA Isolator Level Displacement Results to THA Isolator Level Displacement Results of M-DOF Structure with Benchmark Properties, (a) Soil Type, (b) Peak Ground Acceleration, (c) Story Number, (d) Number of Bays, (e) Radius of Curvature, (f) Isolator Friction

7.2.2.2 Roof Level Displacements

The roof level displacement results and the ratio of the equivalent linear results to the nonlinear analysis are presented in Figure 7.7 and Figure 7.8, respectively.

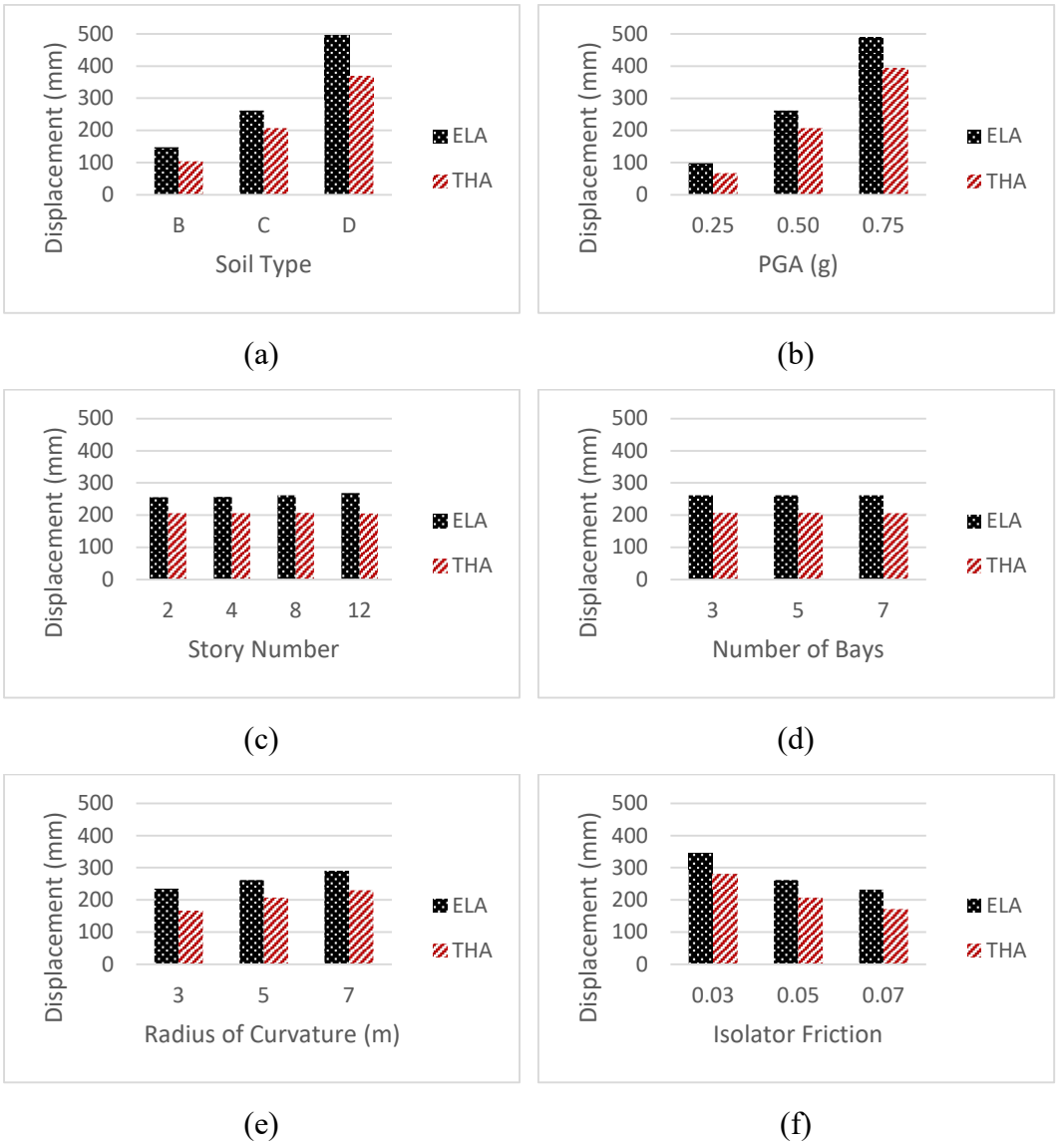

Figure 7.7. Effect of Selected Parameters on the Roof Level Displacement Results for Benchmark Properties, (a) Soil Type, (b) Peak Ground Acceleration, (c) Story Number, (d) Number of Bays, (e) Radius of Curvature, (f) Isolator Friction

The total structural displacement is the difference between the roof displacement and the isolator level displacement. The structural displacements are calculated as 2-3 mm for 2-story buildings, 4-6 mm for 4-story buildings, 10-15 mm for 8-story buildings, and 20-25 mm for 12-story buildings. Those displacements values are quite low due to the base isolation system. In addition, all accuracy results of the roof level are the same as the isolation level displacement results.

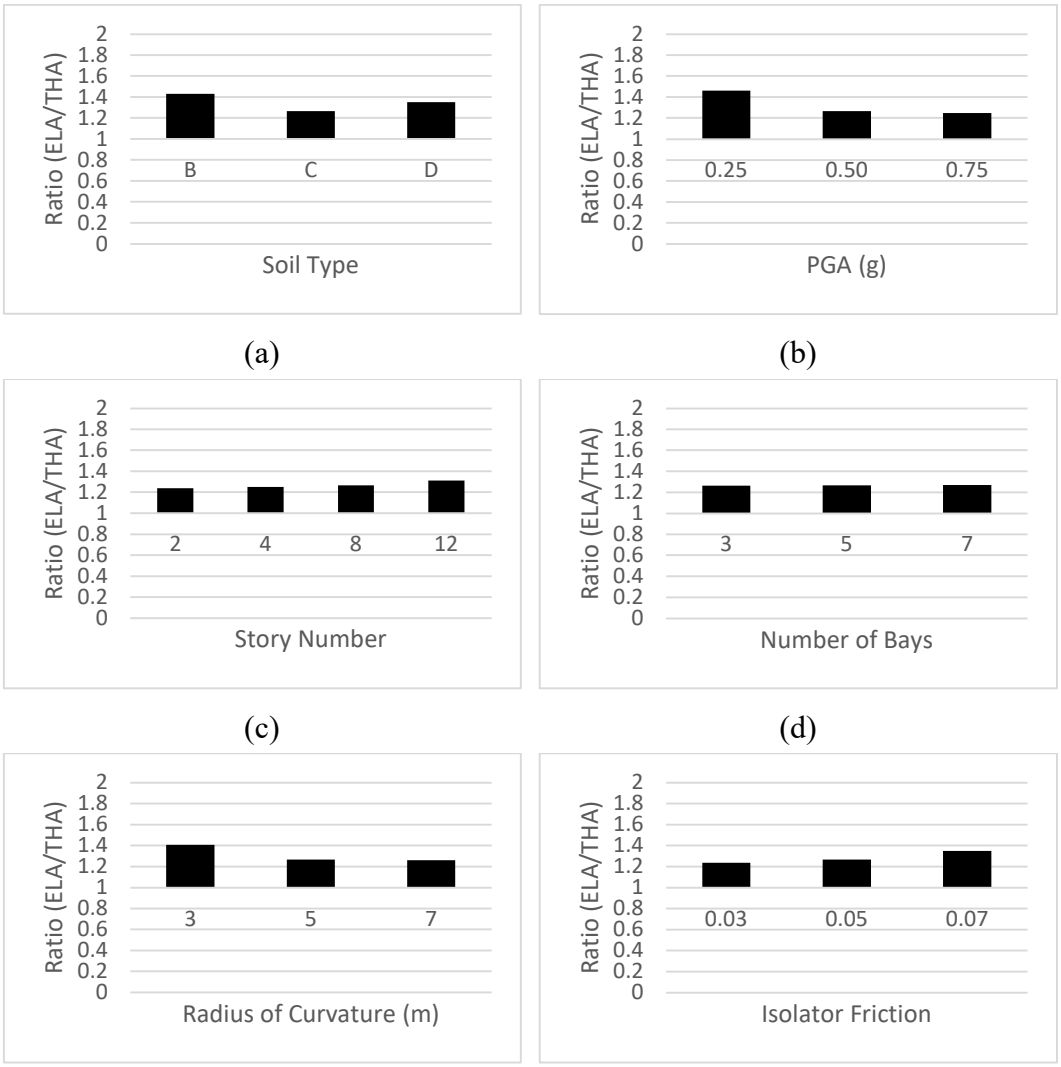

Figure 7.8. Ratio of ELA Roof Level Displacement Results to THA Roof Level Displacement Results of M-DOF Structure with Benchmark Properties, (a) Soil Type, (b) Peak Ground Acceleration, (c) Story Number, (d) Number of Bays, (e) Radius of Curvature, (f) Isolator Friction

7.2.3 Acceleration

Story acceleration is an important criteria for evaluating the earthquake performance of a base-isolated structure, especially for hospitals. In order to evaluate the accuracy of acceleration results for equivalent linear analysis, story acceleration results of the equivalent linear analysis and time history analysis are plotted in the same graph. In addition, the story acceleration results of the fixed-base case are included in the same graph. Story acceleration graphs for the base-isolated and fixed base buildings with benchmark properties are presented in Figure 7.9.

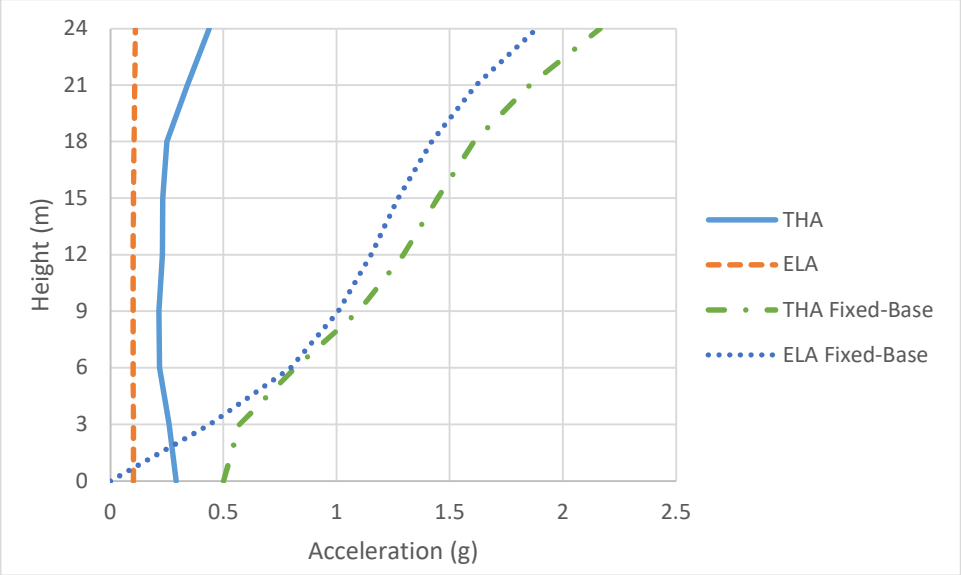

Figure 7.9. Story Accelerations of the Structure With Benchmark Analysis Properties

As observed from the graphs of the nonlinear analysis cases, the story accelerations in the lower floors of the base-isolated building are reduced by half compared to the fixed-base case. This rate increases even more in the upper stories. However, the equivalent linear method underestimates the accelerations up to 60% for the base-isolated case. In order to clearly explain the situation, acceleration results of the equivalent linear analysis are compared with the S-DOF analysis results of the same model, and it is found that the isolator level acceleration results are the same as the

S-DOF acceleration result. This situation implies that the building acts like an S-DOF structure since the main modal mass participation is obtained from the first mode.

7.2.3.1 Effect of Building Parameters on Acceleration

Story acceleration graphs of 3-bay, 5-bay, and 7-bay base-isolated structures are presented in Figure 7.10. As observed from the figure, the bay number of the building does not affect the story accelerations since the story acceleration graphs of 3-bay, 5-bay, and 7-bay buildings are the same.

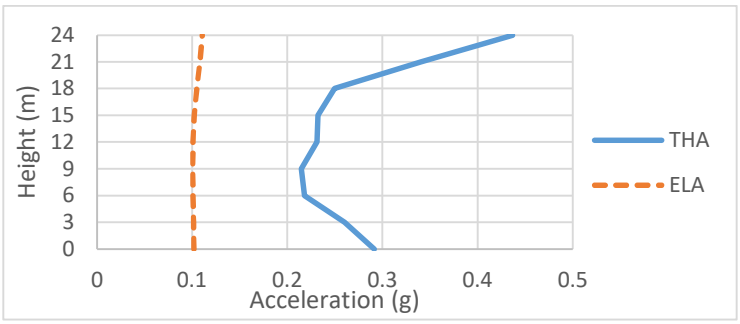

(a)

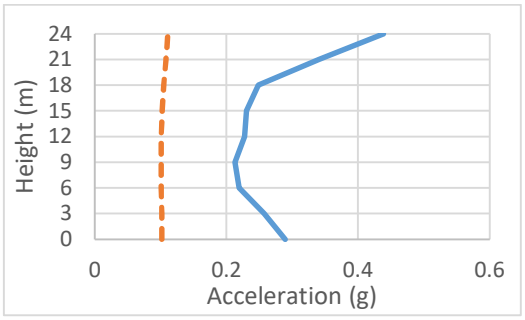

(b)

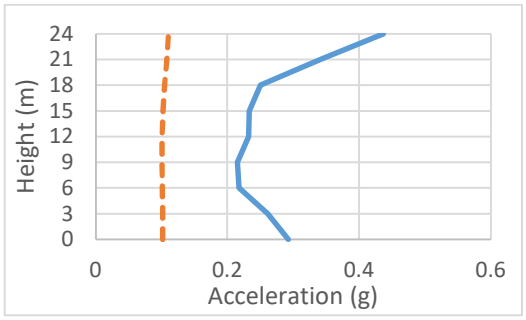

(c)

Figure 7.10. Effect of Bay Number on Story Accelerations Results for Benchmark Properties, (a) 5-Bay, (b) 3-Bay, (c) 7-Bay

The effect of the story number is more complex than the bay number. The story acceleration results of the equivalent linear analysis and S-DOF accelerations are the same for all story numbers, as shown in Figure 7.11. However, the acceleration results of the nonlinear analysis tend to increase as the number of stories of the building increases.

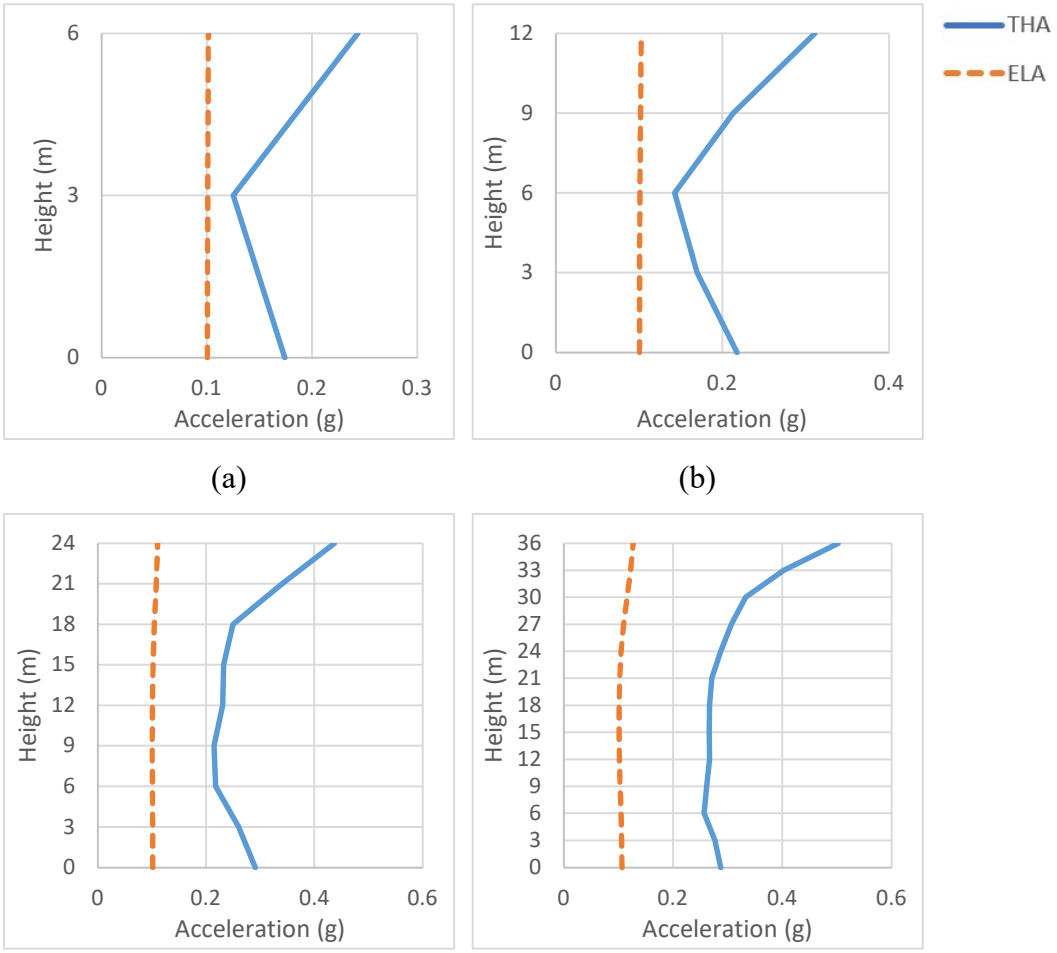

Figure 7.11. Effect of the Story Number on Story Acceleration Results for Benchmark Properties

7.2.3.2 Effect of Isolator Parameters on Acceleration

Story acceleration graphs for different isolator properties are presented in Figure 7.12. The story accelerations at the isolator level of the equivalent linear analysis are quite similar to the S-DOF results for all the isolator parameters. The accuracy of the ELA increases as the friction coefficient decreases and the curvature radius increases since the results of nonlinear analysis gets closer to the equivalent linear analysis.

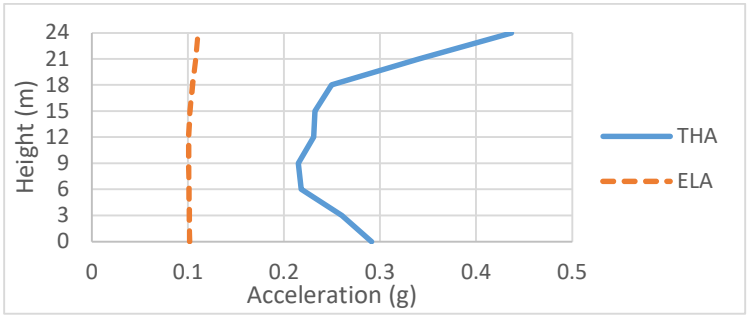

(a)

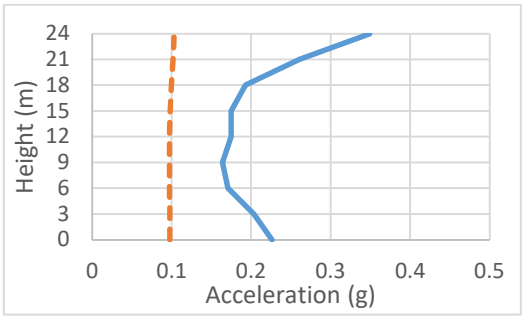

(b)

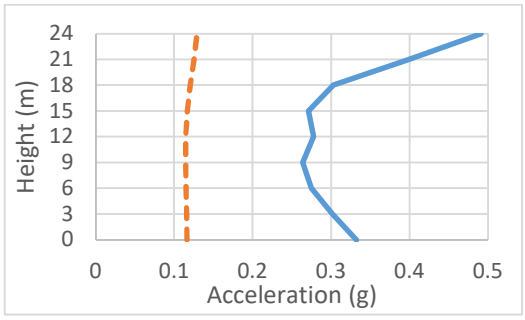

(c)

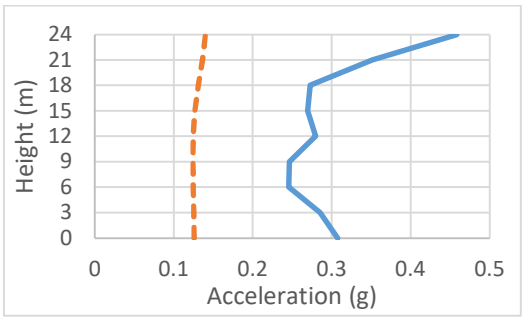

(d)

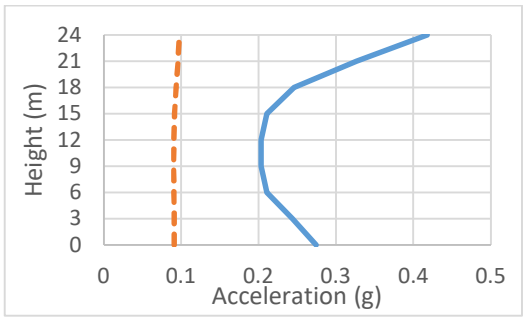

(e)

Figure 7.12. Effect of Isolator Properties on Story Acceleration Results for Benchmark Properties; (a) μ=0.05, R=5; (b) μ=0.03, R=5; (c) μ=0.07, R=5; (d) μ=0.05, R=3; (e) μ=0.05, R=7

7.2.3.3 Effect of Peak Ground Acceleration and Soil Class on Acceleration

The story acceleration graphs for different soil types and peak ground acceleration values are presented in Figure 7.13. Both isolator level acceleration and roof accelerations increase as peak ground acceleration increase and shear wave velocity decreases. However, there is no direct correlation between the accuracy of the equivalent linear method and soil type or peak ground acceleration.

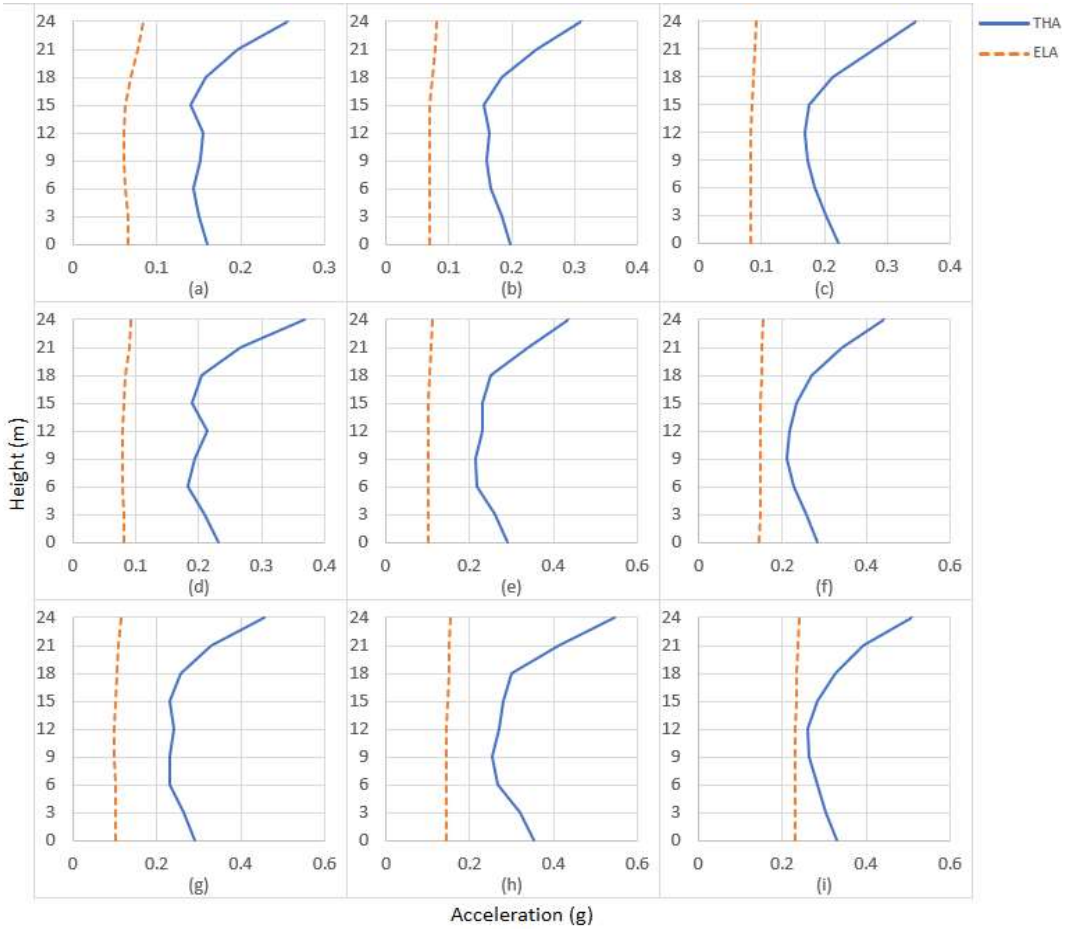

Figure 7.13. Effect of PGA and Soil Site on Base Moment Results for Benchmark Properties; (a) PGA=0.25g, Soil Site Class = B; (b) PGA=0.25g, Soil Site Class = C; (c) PGA=0.25g, Soil Site Class = D; (d) PGA=0.5g, Soil Site Class = B; (e) PGA=0.5g, Soil Site Class = C; (f) PGA=0.5g, Soil Site Class = D; (g) PGA=0.75g, Soil Site Class = B; (h) PGA=0.75g, Soil Site Class = C; (i) PGA=0.75g, Soil Site Class = D

7.2.4 Maximum Interstory Drift Ratio

The inter-story drift ratios are calculated from Eq. 7.1 for each story of a structure. The largest one is presented as the maximum inter-story drift ratio for ELA and THA in Figure 7.14, and their ratio is shown in Figure 7.15.

$$\delta_i = (d_i - d_{i-1}) / H \tag{7.1}$$

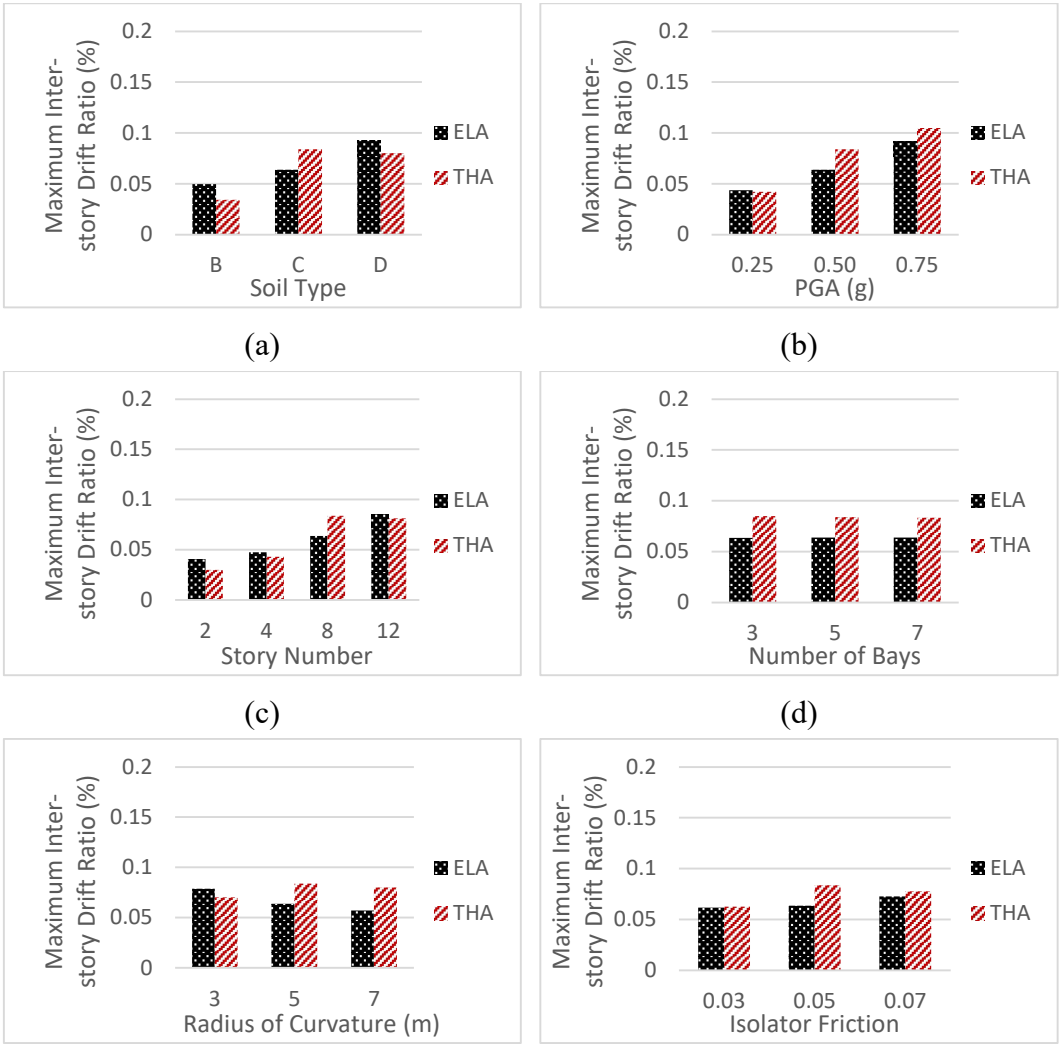

Figure 7.14. Effect of Selected Parameters on the Maximum Inter-story Drift Ratio for Benchmark Properties, (a) Soil Type, (b) Peak Ground Acceleration, (c) Story Number, (d) Number of Bays, (e) Radius of Curvature, (f) Isolator Friction

The results have shown that the maximum inter-story drift ratio increased as the Peak Ground Acceleration increased in both cases. The maximum inter-story drift ratio is calculated as 0.1% for the nonlinear analysis of the structure with benchmark properties and a PGA of 0.75g.

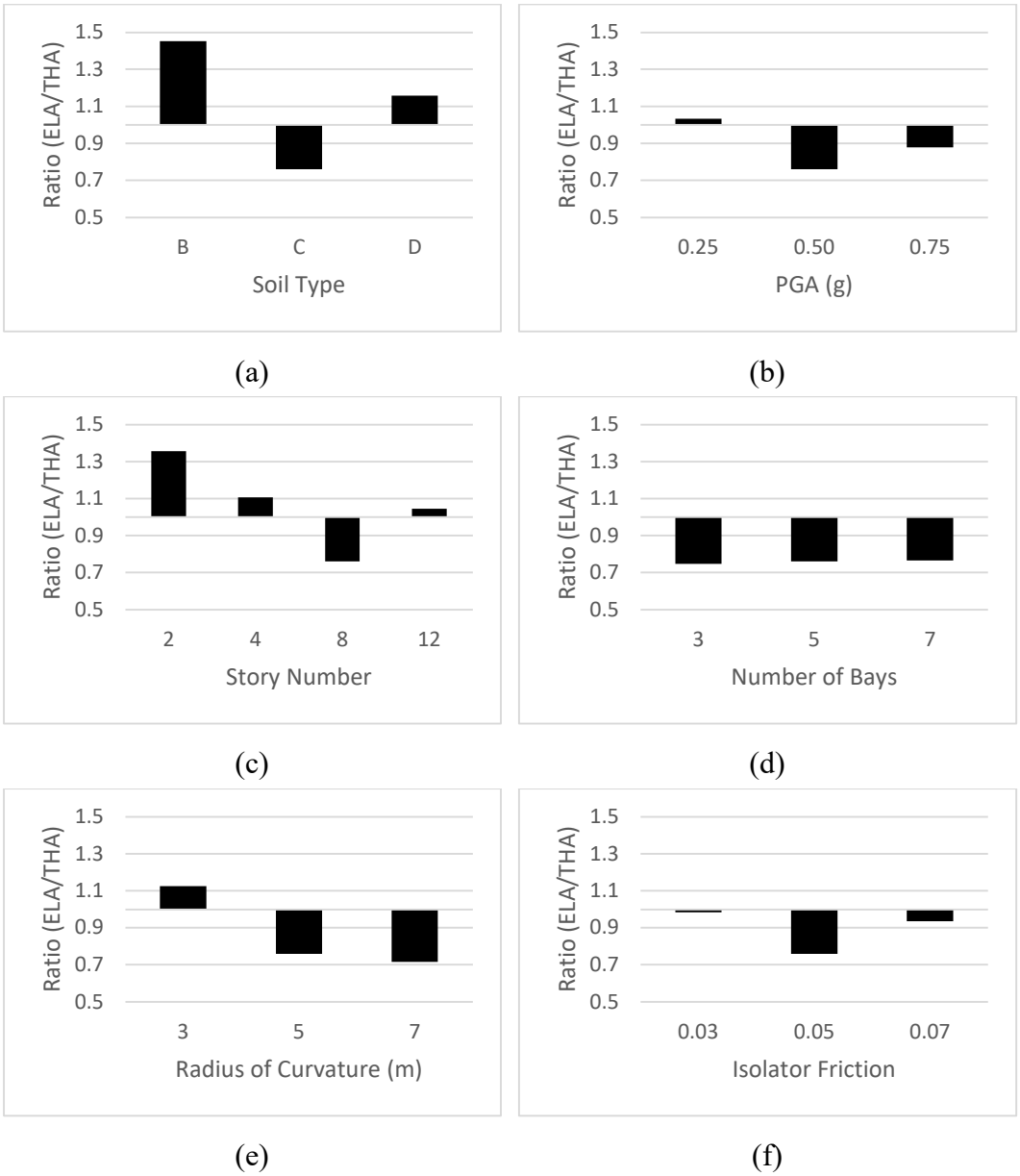

Figure 7.15. Ratio of ELA Maximum Inter-story Drift Ratio Results to THA Maximum Inter-story Drift Ratio Results of M-DOF Structure with Benchmark Properties, (a) Soil Type, (b) Peak Ground Acceleration, (c) Story Number, (d) Number of Bays, (e) Radius of Curvature, (f) Isolator Friction

The equivalent linear method underestimated the maximum inter-story drift results up to 28% and overestimated up to 45%. Since the graphs of 3-bay, 5-bay, and 7-bay buildings are the same, the bay number of the building does not affect the maximum inter-story drift ratio. However, the effect of the other selected parameters on the results was inconclusive since a connection could not be observed.

7.2.5 Column Reactions

Since the earthquake forces significantly affect the outer column of the first story, the axial load and moment results of this column are presented in Figure 7.16 and Figure 7.18, respectively. In addition, the axial load and moment results of the outer and inner columns of the first, mid, and top stories are presented as ratios in Figure 7.17 and Figure 7.19, respectively.

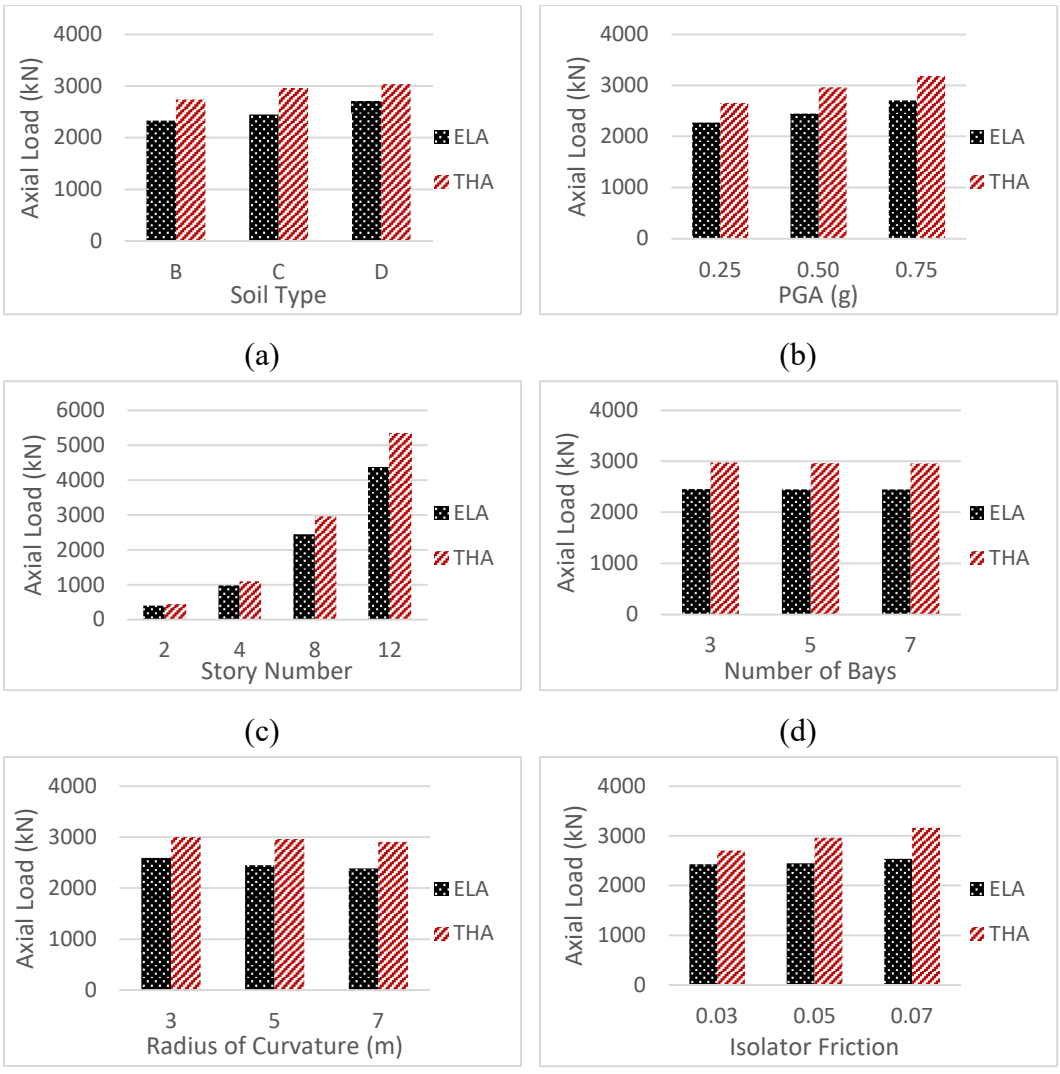

Figure 7.16. Effect of Selected Parameters on Column Axial Load Results for Benchmark Properties, (a) Soil Type, (b) Peak Ground Acceleration, (c) Story Number, (d) Bay Number, (e) Radius of Curvature, (f) Isolator Friction

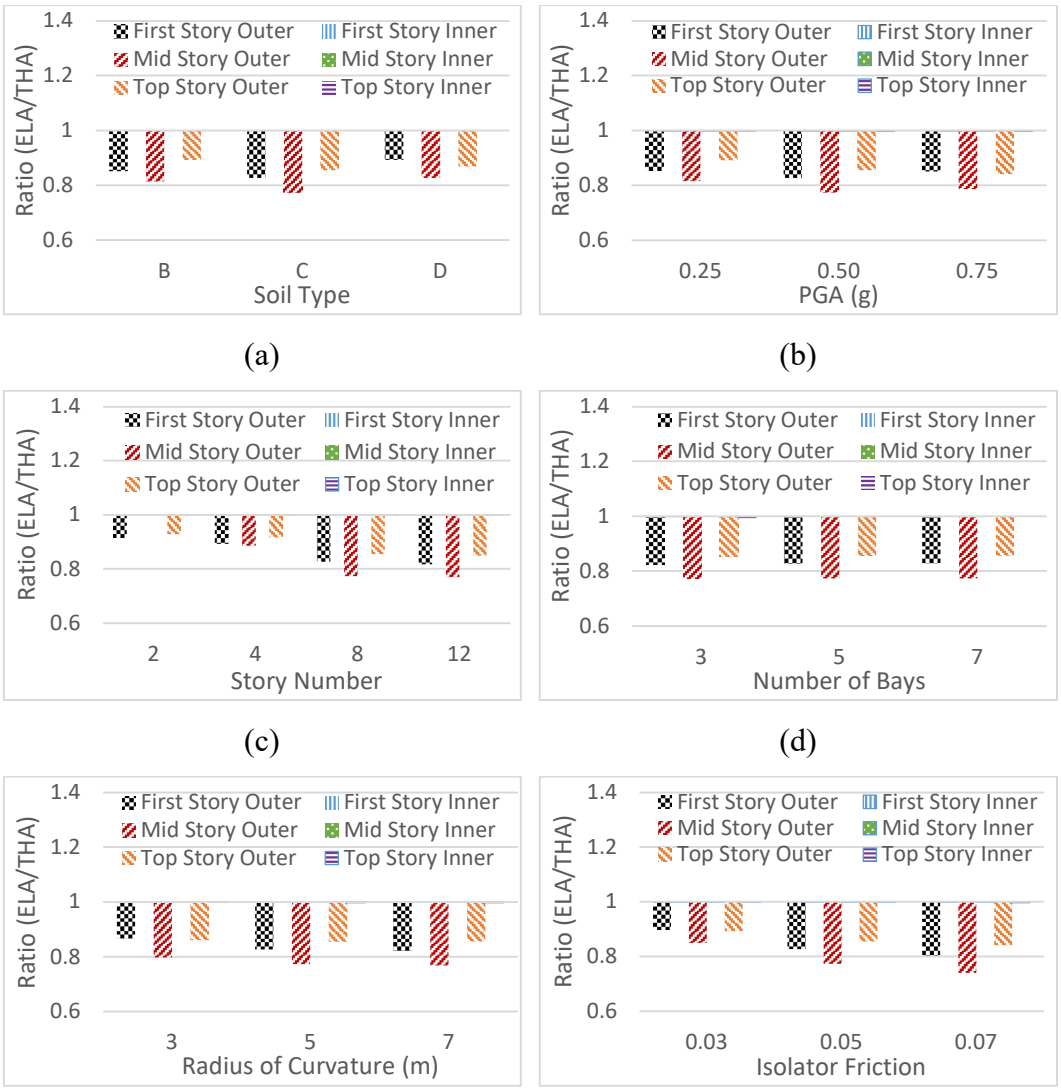

Figure 7.17. Ratio of ELA Column Axial Load Results to THA Column Axial Load Results for Benchmark Properties, (a) Soil Type, (b) Peak Ground Acceleration, (c) Story Number, (d) Number of Bays, (e) Radius of Curvature, (f) Isolator Friction

As observed from the graphs, the equivalent linear method estimates the same axial load with the nonlinear method for the inner columns for all levels. However, the equivalent linear method underestimated the axial loads up to 25% for the outer column of the mid-story. The largest and least underestimations occurred in the mid and top stories, respectively. In addition, the percentage of underestimation

decreases as the isolator friction and the total number of stories decreases. The other parameters are ineffective on the axial load results.

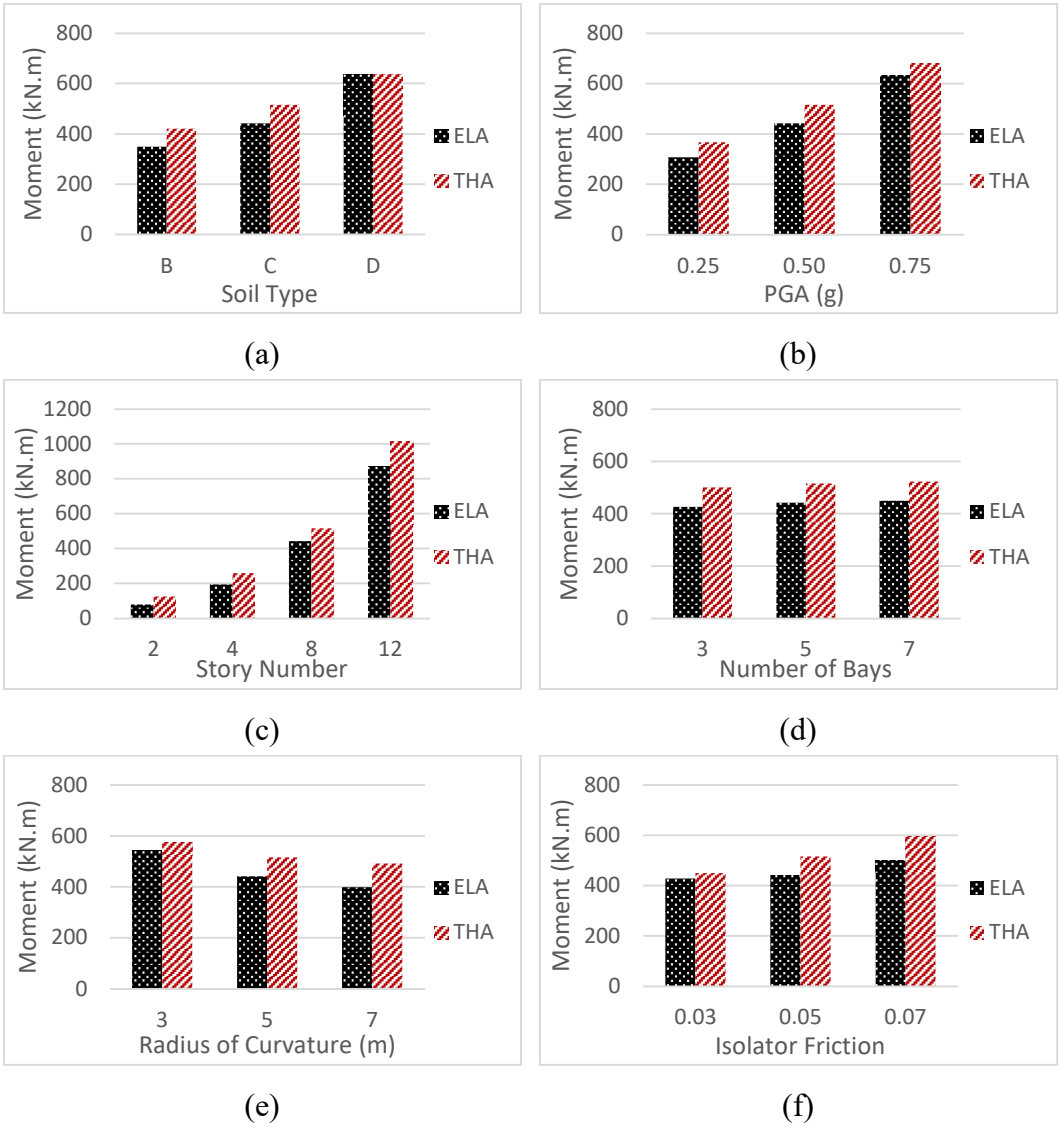

Figure 7.18. Effect of Selected Parameters on Column Moment Results for Benchmark Properties, (a) Soil Type, (b) Peak Ground Acceleration, (c) Story Number, (d) Bay Number, (e) Radius of Curvature, (f) Isolator Friction

On the other hand, the equivalent linear method estimates more accurate moment results for the inner beams than the outer beams. In addition, the moment results of the columns at the first story are much more accurate when compared to the mid and the top stories.

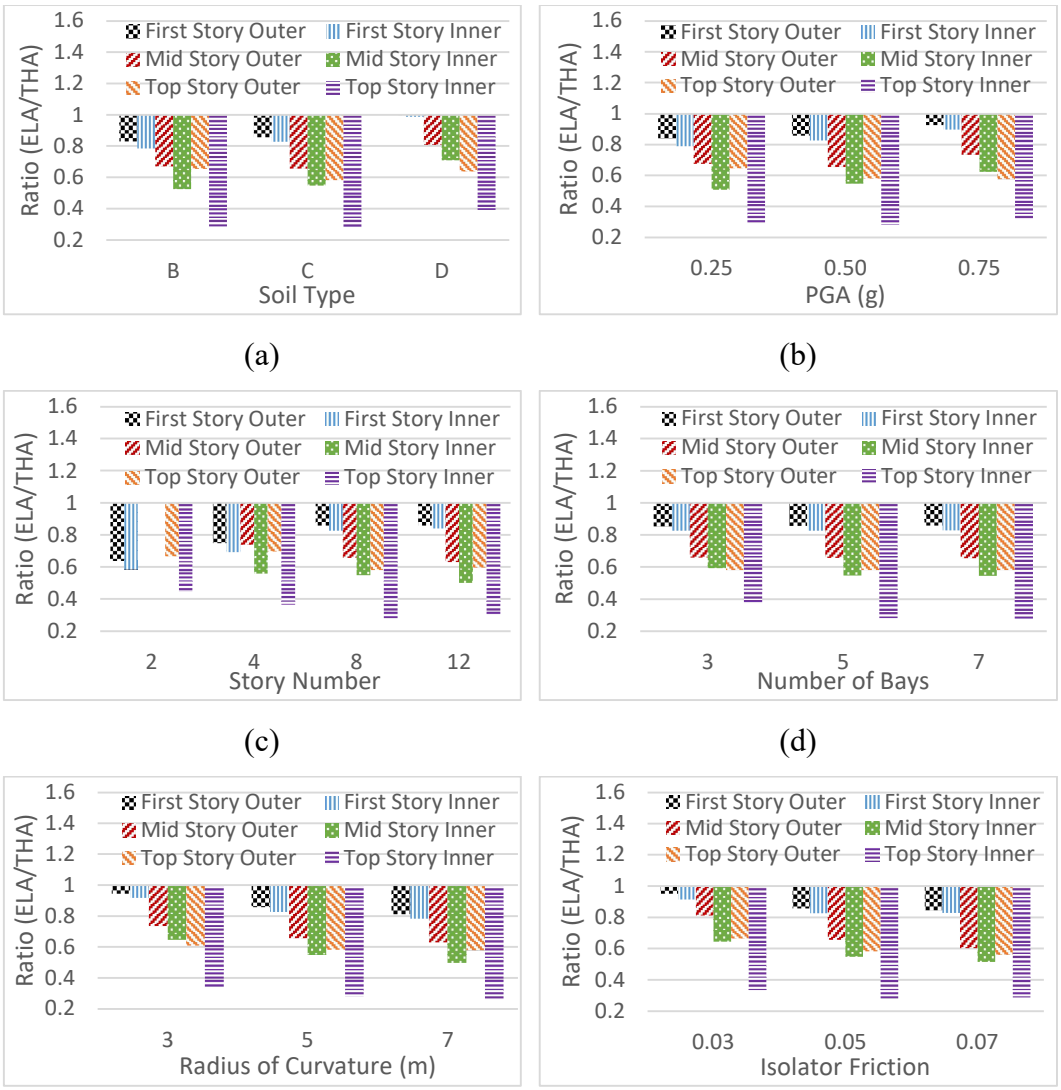

Figure 7.19. Ratio of ELA Column Moment Results to THA Column Moment Results for Benchmark Properties, (a) Soil Type, (b) Peak Ground Acceleration, (c) Story Number, (d) Number of Bays, (e) Radius of Curvature, (f) Isolator Friction

As the total number of stories of the building increase, the accuracy of the results of the first story also increases. However, the accuracy of the results of the top story decreases. The other parameters do not have a significant effect on the moment results.

7.2.6 Beam Reactions

The moment results of the outer beam of the first story and the ratio results of the outer and inner beams of the first, mid, and top stories are presented in Figure 7.20 and Figure 7.21, respectively.

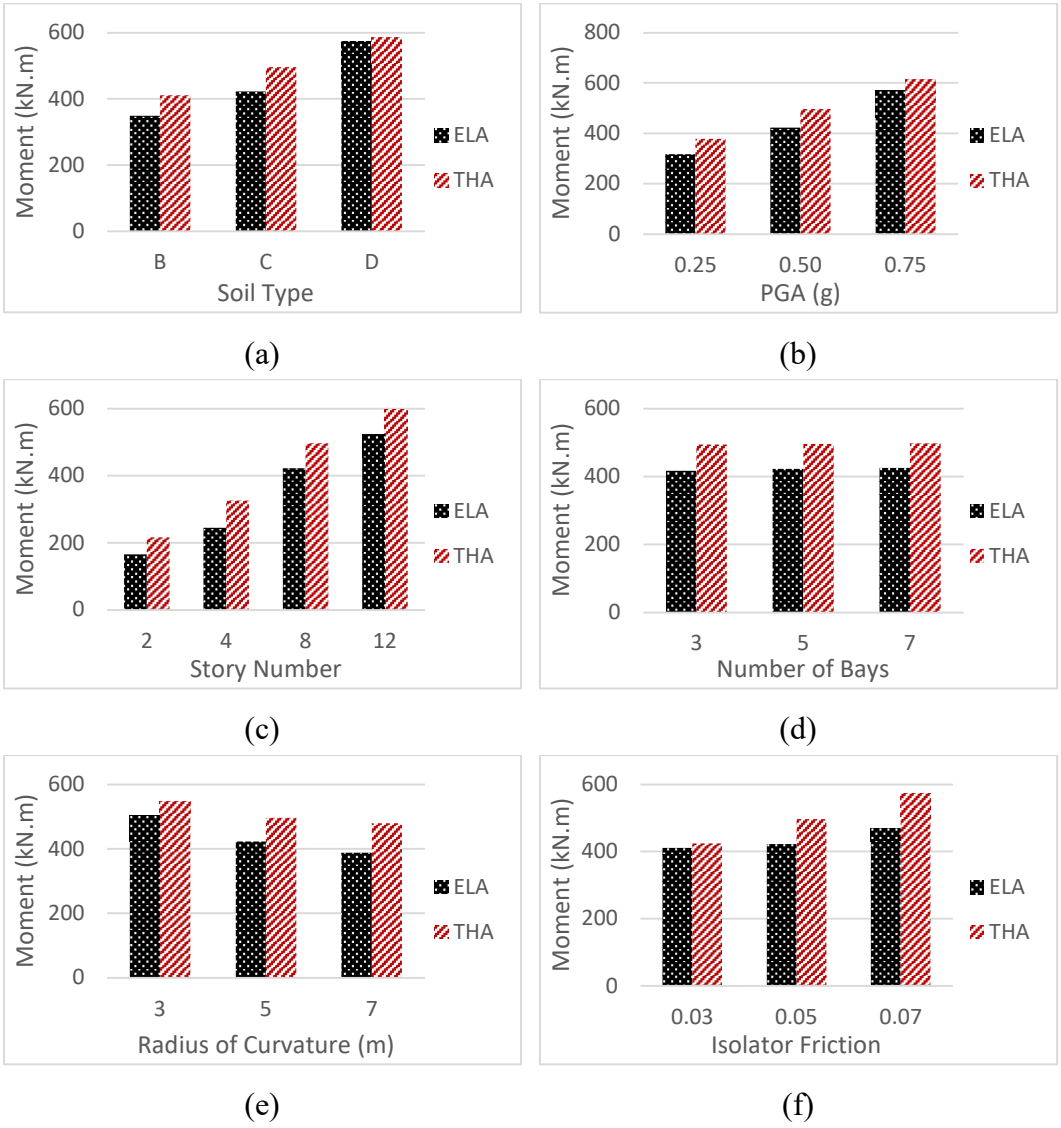

Figure 7.20. Effect of Selected Parameters on Beam Moment Results for Benchmark Properties, (a) Soil Type, (b) Peak Ground Acceleration, (c) Story Number, (d) Bay Number, (e) Radius of Curvature, (f) Isolator Friction

The equivalent linear method estimates very accurate moment results for outer and inner beams of the first story. However, it underestimates the moment results up to 40% for mid and top stories. In addition, the equivalent linear method estimates better results for soil site class D and worse results for soil site class B. Moreover, the accuracy of the results of the first story increases as the peak ground acceleration and the total number of the stories increase. However, it increases as the radius of curvature and the isolator friction decrease.

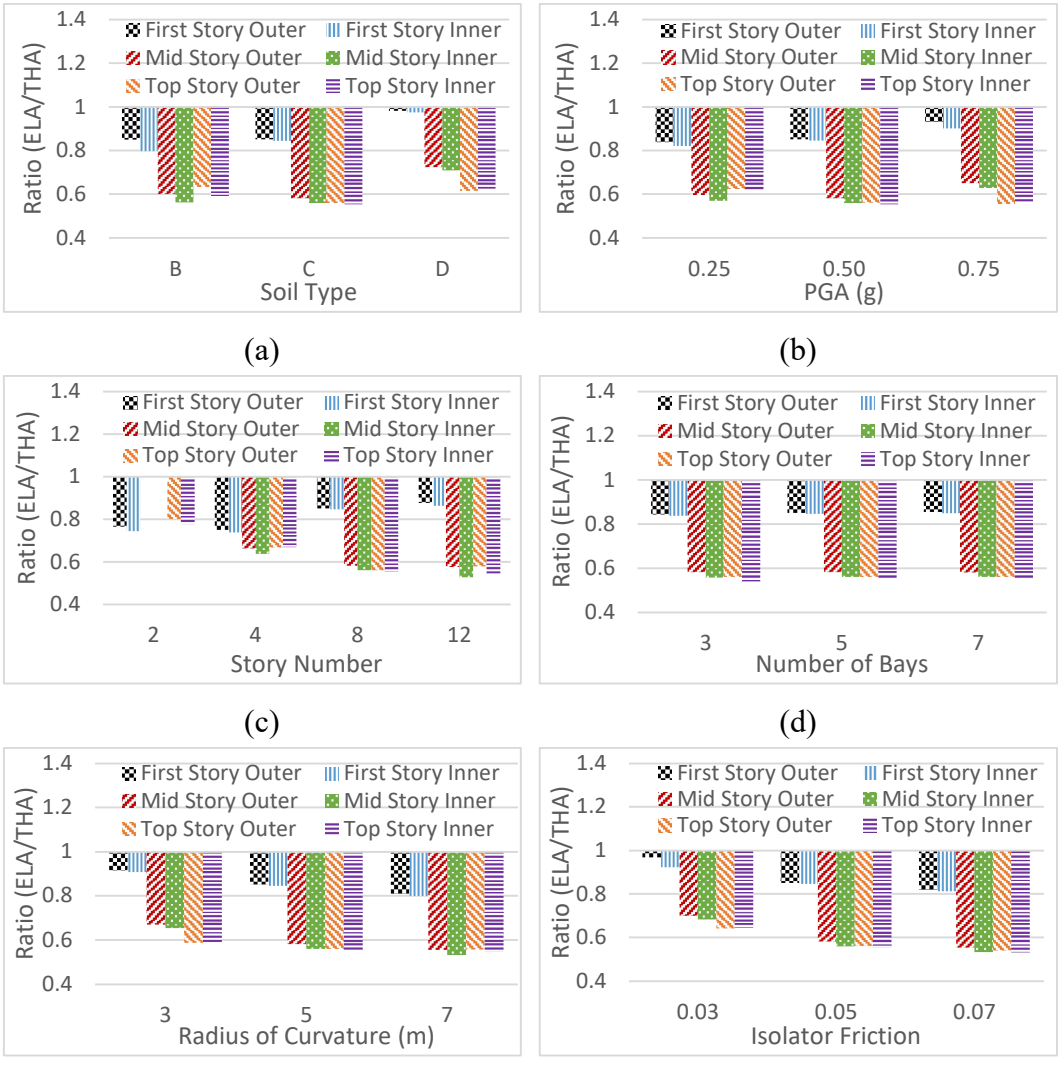

Figure 7.21. Ratio of ELA Beam Moment Results to THA Beam Moment Results for Benchmark Properties, (a) Soil Type, (b) Peak Ground Acceleration, (c) Story Number, (d) Number of Bays, (e) Radius of Curvature, (f) Isolator Friction

CHAPTER 8

CONCLUSION

In this thesis, a parametric study is conducted to evaluate the accuracy of the equivalent linear method for base-isolated structures. Soil site class, peak ground acceleration (PGA), the radius of curvature, isolator friction, number of stories and bays are selected as the main parameters of this study.

The equivalent linear analysis method is easier and faster than the non-linear analysis method. In addition, convergence problem does not occur. In this study, results of ELA are compared with the time history analysis results to see how accurate the method is and how selected parameters affected the accuracy.

A total of 270 analyses are performed for both S-DOF and M-DOF structures using the equivalent linear method. Twice this number of analyses are performed with the nonlinear method to compare Friction Pendulum isolator modeling type and Plastic-Wen isolator modeling type.

The results of S-DOF analyses show that the equivalent linear method estimates accurate results for the acceleration but overestimates the base shear and displacement results up to 20% and 50%, respectively. M-DOF analysis results show a similar level of accuracy with the S-DOF system for the base shear and displacement results. However, the acceleration results are underestimated by more than 50% with the equivalent linear method. In literature, the reason is attributed to the inability of the equivalent linear method to reflect the structural modes for the multi degree of freedom systems. In addition, the analysis program used in this study is based on displacement. Since acceleration is the second derivative of the displacement-time curve, it can be quite difficult to predict acceleration accurately. Moreover, as the degree of freedom of the structure or the time step of the ground motion record increase, it may become even more difficult.

The results found in this study can be concluded as follows:

- The type of link used to model the isolation system affects the results by less than 2%. Friction Isolator link type simulates the behavior more realistically as the variation in stiffness due to the change in axial load during the ground motion is considered.
- Limiting the equivalent damping coefficient only resulted in a worse estimation of the base shear and displacement results. However, better estimations are made for the base moment, acceleration, and all column and beam force results.
- S-DOF and M-DOF analysis results show a similar level of accuracy for the base shear and displacement results. However, the equivalent linear method underestimated the acceleration results for the M-DOF system by more than 50%, whereas the results of the S-DOF system are quite accurate. This difference is caused by the dominance of the first mode due to its high modal mass participation.
- Soil site class has an inconclusive effect on the accuracy of the equivalent linear analysis method.
- Peak ground acceleration has no significant effect on the accuracy of the equivalent linear method, except for the displacement results. As the peak ground acceleration increases, the accuracy of the equivalent linear method for the isolator level displacement and roof level displacement increases.
- As the story number increases, the accuracy of the equivalent linear method for the base moment, acceleration, isolator level, and roof level displacement decreases.
- The number of bays does not affect the accuracy of the equivalent linear method for all selected parameters except for the base moment. As the number of bays increases, the accuracy of the equivalent linear method for the base moment also increases.

- As the radius of curvature increases, the accuracy of the equivalent linear method increases for the base shear and displacement results and decreases for the column and beam forces.
- As the friction constant of the isolator increases, the accuracy of the equivalent linear method decreases for the base moment, displacement, acceleration, column force, and beam force results.
- The accuracy of the equivalent linear method for column and beam force results is mostly higher for the interior and exterior elements of the first floor.

REFERENCES

AASHTO LRFD. (2014). *Bridge Design Specifications*.

Alhan, C., & Özgür, M. (2015). Seismic responses of base-isolated buildings: Efficacy of equivalent linear modeling under near-fault earthquakes. *Smart Structures and Systems*, *15*(6), 1439–1461. https://doi.org/10.12989/sss.2015.15.6.1439

ASCE/SEI 7-16. (2017). *Minimum Design Loads and Associated Criteria for Buildings and Other Structures*, 1–889. https://doi.org/10.1061/9780784414248

Dicleli, M., & Buddaram, S. (2007). Comprehensive evaluation of equivalent linear analysis method for seismic-isolated structures represented by sdof systems. *Engineering Structures*, *29*(8), 1653–1663. https://doi.org/10.1016/j.engstruct.2006.09.013

Dicleli, M., & Mansour, M. Y. (2003). Seismic retrofitting of highway bridges in Illinois using friction pendulum seismic isolation bearings and modeling procedures. *Engineering Structures*, *25*(9), 1139–1156. https://doi.org/10.1016/S0141-0296(03)00062-2

Gino, D., Anerdi, C., Castaldo, P., Ferrara, M., Bertagnoli, G., & Giordano, L. (2020). Seismic upgrading of existing reinforced concrete buildings using friction pendulum devices: A probabilistic evaluation. *Applied Sciences (Switzerland)*, *10*(24), 1–17. https://doi.org/10.3390/app10248980

Kim, S. Y. (2017). *Evaluation of Equivalent Linear Methods for Seismic Response Analysis of Base Isolated Structures*.

Liu, T., Zordan, T., Briseghella, B., & Zhang, Q. (2014a). Simplified linear static analysis for base-isolated buildings with friction pendulum systems. *Structural Engineering International: Journal of the International Association for Bridge*

and Structural Engineering (IABSE), *24*(4), 490–502. https://doi.org/10.2749/101686614X13854694314405

Liu, T., Zordan, T., Briseghella, B., & Zhang, Q. (2014b). An improved equivalent linear model of seismic isolation system with bilinear behavior. *Engineering Structures*, *61*, 113–126. https://doi.org/10.1016/j.engstruct.2014.01.013

Lousidis, A. P. (2015). *Technical University of Crete Dynamic Analysis of a Friction Pendulum Isolation System (FPS) under earthquake excitation Declaration of Authorship*. *September*.

Nagarajaiah, S., Reinhorn, A. M., & Constantinou, M. C. (1991). *NONLINEAR DYNAMIC ANALYSIS OF 3-D-BASE-ISOLATED STRUCTURES*.

Nguyen, T.-T., & Dao, N. D. (2021). Evaluating the Accuracy of an Equivalent Linear Model in Predicting Peak Displacement of Seismic Isolation Systems using Single Friction Pendulum Bearings. *Periodica Polytechnica Civil Engineering*. https://doi.org/10.3311/PPci.17687

Ozdemir, G., & Constantinou, M. C. (2010). Evaluation of equivalent lateral force procedure in estimating seismic isolator displacements. *Soil Dynamics and Earthquake Engineering*, *30*(10), 1036–1042. https://doi.org/10.1016/j.soildyn.2010.04.015

Pant, D. R., Wijeyewickrema, A. C., & ElGawady, M. A. (2013). Appropriate viscous damping for nonlinear time-history analysis of base-isolated reinforced concrete buildings. *Earthquake Engineering and Structural Dynamics*, *42*(15), 2321–2339. https://doi.org/10.1002/eqe.2328

Ryan, K. L., & Polanco, J. (2008). *Problems with Rayleigh Damping in Base-Isolated Buildings*. https://doi.org/10.1061/ASCE0733-94452008134:111780

SAP2000 v22. (2020). *Computers and Structures INC.*

Siciliano, A. (2016). *Ageing Effects on Seismic Isolation Devices*.

Simon, J., Vigh, L. G., Horváth, A., & Pusztai, P. (2015). Application and assessment of equivalent linear analysis method for conceptual seismic retrofit design of Háros M0 highway bridge. *Periodica Polytechnica Civil Engineering*, *59*(2), 109–122. https://doi.org/10.3311/PPci.7860